Protective effects of the neuropeptides PACAP, substance P and the somatostatin analogue octreotide in retinal ischemia: a metabolomic analysis

Journal:	*Molecular BioSystems*
Manuscript ID:	MB-ART-08-2013-070362.R1
Article Type:	Paper
Date Submitted by the Author:	n/a

Complete List of Authors:	D'Alessandro, Angelo; Tuscia University, Department of Ecological and Biological Sciences Cervia, Davide; Tuscia University, Dipartimento per l'Innovazione nei Sistemi Biologici, Agroalimentari e Forestali Catalani, Elisabetta; Tuscia University, Dipartimento per l'Innovazione nei Sistemi Biologici, Agroalimentari e Forestali Gevi, Federica; Tuscia University, Department of Ecological and Biological Sciences Zolla, Lello; Tuscia University, Dpt. of Environmental Sciences Casini, Giovanni; Università di Pisa, Dipartimento di Biologia

Protective effects of the neuropeptides PACAP, substance P and the somatostatin analogue octreotide in retinal ischemia: a metabolomic analysis

Angelo D'Alessandro[a], Davide Cervia[b,c],Elisabetta Catalani[b], Federica Gevi[a], Lello Zolla[a,*], Giovanni Casini[d,*]

[a]Dipartimento di Scienze Ecologiche e Biologiche, Università della Tuscia, I-01100 Viterbo, Italy

[b]Dipartimento per l'Innovazione nei Sistemi Biologici, Agroalimentari e Forestali, Università della Tuscia, I-01100 Viterbo, Italy

[c]Dipartimento di Scienze Biomediche e Cliniche "Luigi Sacco", Università di Milano, I-20157 Milano, Italy

[d]Dipartimento di Biologia, Università di Pisa, I-56127 Pisa, Italy

* Corresponding authors at:

Giovanni Casini - gcasini@biologia.unipi.it Dipartimento di Biologia, Università di Pisa, via S. Zeno 31, 56127, Pisa, Italy. Tel.: +39 050 2211423; Fax: +39 050 2211421

Lello Zolla – zolla@unitus.it Dipartimento di Scienze Ecologiche e Biologiche, Università della Tuscia, L.go dell'Università snc, 01100, Viterbo, Italy. Tel.: +39 0761 357100; Fax: +39 0761 357179

E-mail addresses: a.dalessandro@unitus.it (A. D'Alessandro), d.cervia@unitus.it (D. Cervia), ecatalani@unitus.it (E. Catalani), gevi@unitus.it (F. Gevi), zolla@unitus.it (L. Zolla), gcasini@biologia.unipi.it (G. Casini).

Running title: Metabolomics of the peptide-treated ischemic retina

---

Abbreviations: DAPI, 4'-6-diamidino-2-phenylindole; DPG, 2,3-diphosphoglycerate; ESI, electrospray ionization; G3P, glyceraldehyde 3-phosphate; GAPDH, Glyceraldehyde 3-phosphate dehydrogenase; GCL, ganglion cell layer; GSH, glutathione; GSSG, oxidized glutathione; INL, inner nuclear layer; IP3, inositol triphosphate; IPL, inner plexiform layer; MRM, multiple reaction monitoring; MS, mass spectrometry; NO, nitric oxide; OCT, octreotide; ONL, outer nuclear layer; OPL, outer plexiform layer; PACAP, pituitary adenylate cyclase activating peptide; PB, phosphate buffer; PBS, phosphate-buffered saline; PEP, phosphoenolpyruvate; PIP2, phosphatidyl-inositol 4,5 phosphate; PIP3, phosphatidyl-inositol 3,4,5-triphosphate; PKA, protein kinase A; PPP, pentose phosphate pathway; ROS, reactive oxygen species; SP, substance P; VEGF, vascular endothelial growth factor

Abstract

Ischemia is a primary cause of neuronal death in retinal diseases and the somatostatin subtype receptor 2 agonist octreotide (OCT) is known to decrease ischemia-induced retinal cell death. Using a recently optimized *ex vivo* mouse model of retinal ischemia, we tested the anti-ischemic potential of two additional neuropeptides, pituitary adenylate cyclase activating peptide (PACAP) and substance P (SP), and monitored the major changes occurring at the metabolic level.

Metabolomics analyses were performed via fast HPLC online with a microTOF-Q MS instrument, a workflow that is increasingly becoming the gold standard in the field of metabolomics.

The metabolomic approach allowed detection of the most significant alterations induced in the retina by ischemia and of the significance of the protective effects exerted by OCT, PACAP or SP. All treatments were shown to reduce ischemia-induced cell death, vascular endothelial growth factor over-expression and glutamate release. The metabolomic analysis showed that OCT and, to a lesser extent, also PACAP or SP, were able to counteract the ischemia-induced oxidative stress and to promote, with various efficacy, (i) a decreased accumulation of glutamate and normalization of glutathione homeostasis; (ii) a reduced build-up of α-ketoglutarate, that might serve as a substrate for the enhanced biosynthesis of glutamate in response to ischemia; (iii) a reduced accumulation of peroxidized lipids and inflammatory mediators; (iv) the normalization of glycolytic fluxes and thus prevented the over-accumulation of lactate, or either promoted the down-regulation of the glyoxalate anti-oxidant system; (v) a reduced metabolic shift from glycolysis towards the PPP or either a blockade at the non-oxidative phase of the PPP; (vi) tuning down of purine metabolism.

In addition, OCT seemed to stimulate nitric oxide production. None of the treatments was able to restore ATP production, although ATP reservoirs were partly replenished by OCT, PACAP or SP.

These data indicate that, in addition to that of somatostatin, peptidergic systems such as those of PACAP and SP deserve attention in view of peptide-based therapies to treat ischemic retinal disorders.

Keywords: neuropeptides, cell death, glutamate, mass spectrometry, metabolic shift, mouse retina.

Introduction

Retinal ischemia is cause of visual impairment and blindness. It is assumed to be involved in the pathogenesis of major vision-threatening diseases, such as age-related macular degeneration, diabetic retinopathy and glaucoma[1,2]. It consists in a reduction of blood supply leading to decreased oxygen availability and nutrient delivery, other than to limited or no removal of damaging cellular metabolites.[2]. Ischemia is also the driving force for new vessel formation in the retina,[3] which is observed in retinal diseases such as proliferative diabetic retinopathy, retinopathy of prematurity, central vein occlusion and branch retinal vein occlusion[4]. Studies in animal models have been helpful in suggesting therapeutic strategies; however it is essential to further our understanding of the molecular events taking place downstream of the proposed therapeutic drugs.

Recently, using an *ex vivo* model of the ischemic mouse retina, we provided evidence for the presence of apoptosis in the retinal layers and for the positive correlation of the ischemic damage with glutamate release. Owing to this model, we could determine a role for the neuropeptide somatostatin in the rescue of retinal cells from ischemic damage[5,6]. In particular, it has been established that activation of somatostatin subtype 2 (sst_2) receptors by somatostatin or its analog octreotide (OCT), a sst_2 receptor-preferring agonist, protects retinal neurons against ischemia-induced damage[5-12].

The therapeutic potential of natural substances such as neuropeptides or their analogs resides in the multiplicity of peptidergic receptors and of the transduction pathways they activate. Peptides display high specificity for their receptors and have minimal cross-reactivity. Different from other small molecule therapeutics, peptides do not accumulate in tissues and they are efficiently metabolized by endogenous enzymes. They also have only limited potential for drug-drug interactions and are free of important toxicological complications[13]. In addition to that of somatostatin, other peptidergic systems deserve to be exploited for their possible protective effects against retinal ischemia. For instance, pituitary adenylate cyclase activating polypeptide (PACAP) is known to protect the retina against a variety of insults and anti-ischemic actions have been reported for PACAP[8,14,15]. Neuroprotective mechanisms mediated by PACAP are likely to stem from its potent anti-oxidant, anti-inflammatory and anti-apoptotic effects[15]. Substance P (SP) may be another neuropeptide of interest for potential anti-ischemic properties[8,14]. Its levels are known to increase in response to cerebral ischemia[16] and SP has been reported to mediate retinal responses to acute myocardial ischemia[17].

In the present study, we investigated the effects of OCT, PACAP or SP treatments in an *ex vivo* model of retinal ischemia similar to that used in previous studies[5,6,9]. Subsequently, an in-depth metabolomic investigation of the comprehensive changes at the metabolic level (low molecular weight compounds < 1.5 kDa) was performed through the application of innovative HPLC-mass spectrometry (MS) approaches. MS-based metabolomics has recently gained momentum and became to be considered the apogee of the omics trilogy as an ideal complement to genomics and proteomics[18]. Metabolomics represents a paradigm shift in metabolic research, away from approaches that focus on a limited number of enzymatic reactions or single pathways, to approaches that attempt to capture the complexity of metabolic networks. We could hereby take advantage of an analytical approach that we recently set up[19,20] and successfully applied to a wide series of biological matrices[21-23]. The use of these novel functional tools to study metabolic effects of neuropeptides provides a unique insight into the progression of retinal ischemic disease.

Materials and methods

Animals and applied drugs

Experiments were performed on retinas of C57BL⁄6 mice of both sexes in compliance with the Italian law on animal care N° 116⁄1992 and in accordance with the European Community Council Directive (EEC⁄609⁄86). In all experiments, mice were anaesthetized by i.p. injection of Avertin (1.2% tribromoethanol and 2.4% amylene hydrate in distilled water, 0.02 mL⁄g body weight; Sigma Aldrich, St Louis, MO, USA) and killed by cervical dislocation. The retinas were rapidly dissected in phosphate-buffered saline (PBS – standard solution both containing sodium and potassium salts, Na_2HPO_4 and KH_2PO_4) and subjected to ischemic treatment or incubated in control conditions, in the absence or in the presence of OCT, PACAP-38 or SP. OCT was a gift of Prof. D. Hoyer and Dr H. Schmid (Novartis Pharma, Basel, Switzerland); PACAP-38 (referred to as PACAP in the remainder of the paper) and SP were purchased from Sigma. All treatments were performed at the same time of the day (between 09:00 h and 15:00 h) in order to exclude possible circadian influences. Data collected from both male and female mice were combined, since there was no apparent gender difference.

Ex vivo *ischemic treatment and drug administration*

In preliminary experiments, we verified that a metabolomic analysis was difficult in the ischemic model that we have set up for use in our previous work[5,6,9]. Therefore, we designed a different

ischemic treatment in which the dissected retinas were incubated for 30 minutes, 1 hour or 3 hours at 37°C in N_2-saturated PBS containing 1 mM sodium azide in airtight vials (ischemic treatment) or in air-saturated PBS containing 6 mm glucose in open vials (non-ischemic control). Experiments were conducted in order to set the conditions of the ischemic treatment to obtain a significant score of cell death, as determined with the TUNEL technique, in all three nuclear layers, i.e. the outer nuclear layer (ONL), the inner nuclear layer (INL) and the ganglion cell layer (GCL). A significant cell death was observed in retinas incubated in ischemic conditions for 3 hours (see results), therefore the effects of OCT, PACAP or SP were investigated in retinas treated with the ischemic solution for 3 hours.

OCT and SP were applied at 1 μM, while PACAP was applied at 0.1 μM concentration, at the beginning of the incubation period. According to previous studies, 1 μM OCT is a concentration giving maximal receptor occupancy in different systems[24], including mouse retina[25,26]; 1 μM SP is a concentration within the range of those applied in rodent brain slices *in vitro* (0.75 - 4.0 μM[27-29]); 0.1 μM PACAP is in the range of concentrations previously used *in vitro* to evaluate PACAP neuroprotective effects in developing rat retinas (100 fM - 1 μM[30,31]).

Preparation of retinal sections, TUNEL staining and quantitative analysis

At the end of the incubation period, the retinas used for the TUNEL staining were immersion fixed in 4% paraformaldehyde in 0.1 m phosphate buffer (PB) for 45 to 60 min at room temperature and stored overnight in 25% sucrose in 0.1 m PB at 4 °C. Retinal sections were cut perpendicularly to the vitreal surface at 10 μm with a cryostat, mounted onto gelatin-coated slides and stored at -20°C. All retinas were cut with the same temporal-to-nasal orientation. Consecutive sections were alternately put onto a series of five slides, so that on each slide the sections were spaced every 50 μm. Five sections were put on each slide, and five series of slides were prepared from each retina. Corresponding series of the different experimental conditions were used in each experiment. At least three retinas were analyzed for each experimental condition and at least two series of slides from each retina were used for the TUNEL staining.

An in situ cell death detection kit (Roche Diagnostics, Basel, Switzerland) was used to identify apoptotic profiles by TUNEL technique according to the manufacturer's instructions. The slides were coverslipped in a 0.1 m PB-glycerin mixture containing 0.5 μg/mL of 4'-6-diamidino-2-phenylindole (DAPI, Sigma). TUNEL images were acquired using a 40X plan-NEOFLUAR Zeiss objective, an Axiocam photocamera and the Zeiss Axiovision 4 software. The digital images were

sized and optimized for contrast and brightness using Adobe Photoshop. Final images were saved at a minimum of 300 dpi. The fluorescent TUNEL staining was evaluated in selected sections to calculate the percentage of cell death in each nuclear layer of the retina, as previously described[5,6].

qPCR assay

qPCR experiments were performed in agreement with previous reports[10]. Briefly, total RNA was extracted from 3 retinas per experimental condition with the RNeasy Mini Kit and DNAse digestion (Qiagen, Valencia, CA, USA), according to the manufacturer's instructions. After solubilization in RNase-free water, total RNA was quantified by Picodrop Microlitre Spectrophotometer (Picodrop, Saffron Walden, UK). First-strand cDNA was generated from 3 μg of total RNA using ImProm-II Reverse Transcription System (Promega, Madison, WI, USA). As shown in **Table 1**, primer pairs amplifying 69-172 bp fragments were designed to hybridize to unique regions of the appropriate gene sequence. qPCR was performed using Brilliant SYBR Green Q-PCR Master Mix (M-Medical, Milan, Italy) according to the manufacturer's recommended procedure. All reactions were run in triplicates and the template was replaced with water in all blank control reactions. The fluorescence was read during the reaction by Mx3000PTM real time PCR system (Stratagene, La Jolla, CA, USA), allowing a continuous monitoring of the amount of PCR products. The melt-curve analysis was performed at the end of each experiment to verify that a single product per primer pair was amplified. As to control experiments, gel electrophoresis was also performed to verify the specificity and the size of the amplified qPCR products (**Suppl. Fig.1**). The analysis was carried out using the endpoints method option that causes the collection of the fluorescence data at the end of each extension stage of amplification. Samples were compared using the relative cycle threshold method. The fold increase or decrease was determined relative to a control after normalizing to Glyceraldehyde 3-phosphate dehydrogenase (GAPDH, internal standard) through the use of the formula $2^{-\Delta\Delta CT}$[32].

Statistical analysis of the TUNEL and qPCR data

Upon verification of normal distribution, statistical significance of raw data between the groups in each experiment was evaluated using ANOVA followed by the Newman-Keuls Multiple Comparison post-test. The GraphPad Prism software package (GraphPad Software, San Diego, CA, USA) was used. After statistics (raw data), data belonging from different experiments were represented and averaged in the same graph. The results were expressed as means ± SEM.

Untargeted Metabolomic Analyses

Metabolite extraction

Metabolomic analyses were performed as previously reported[19,20], with minor modifications. Triplicate runs were performed on five retinas for each of the five groups (non-ischemic control, ischemic, ischemic treated with OCT, PACAP or SP). Samples were extracted following a validated protocol[19,33]. Retinas were resuspended in 0.15 mL of ice cold ultra-pure water (18 MΩ) to lyse cell, then the tubes were plunged into a water bath at 37°C for 0.5 min. Samples were mixed with 0.6 mL of -20°C methanol and then with 0.45 mL chloroform. Subsequently, 0.15 mL of ice cold ultra-pure water were added to each tube and the tubes were transferred to -20°C for 2-8 hours. An equivalent volume of acetonitrile was added to the tube and transferred to refrigerator (4°C) for 20 min. Samples with precipitated proteins were thus centrifuged for 10000 x g for 10 min at 4 °C. Finally, samples were dried in a rotational vacuum concentrator (RVC 2-18 - Christ Gmbh, Osterode am Harz, Germany) and resuspended in 200 µl of 5% formic acid and transferred to glass auto-sampler vials for LC/MS analysis.

Rapid Resolution Reversed-Phase HPLC

An Ultimate 3000 Rapid Resolution HPLC system (LC Packings, Dionex, Sunnyvale, CA, USA) was used to perform metabolite separation. The system featured a binary pump and vacuum degasser, well-plate autosampler with a six-port micro-switching valve, a thermostated column compartment. Samples were loaded onto a Reprosil C18 column (2.0 mm of i.d. × 150 mm of length and particle size 2.5 µm, 100 Å pore diameter/surface area, 17% C – r125.b9.s1502, DrMaisch, Ammerbuch-Entringen, Germany) for metabolite separation. Chromatographic separations were achieved at a column temperature of 30°C; and flow rate of 0.2 mL/min. For downstream negative ion mode (-) MS analyses, A 0–100% linear gradient of solvent A (10 mM tributylamine aqueous solution adjusted with 15 mM acetic acid, pH 4.95) to B (methanol mixed with 10 mM TBA and with 15 mM acetic acid, pH 4.95) was employed over 30 min, returning to 100% A in 2 minutes and a 6-min post-time solvent A hold. For downstream positive ion mode (+) MS analyses, a 0–100% linear gradient of solvent A (ddH_2O, 0.1% formic acid) to B (acetonitrile, 0.1% formic acid) was employed over 30 min, returning to 100% A in 2 minutes and a 6-min post-time solvent A hold.

Mass Spectrometry: Q-TOF settings

Due to the use of linear ion counting for direct comparisons against naturally expected isotopic ratios, time-of-flight instruments are most often the best choice for molecular formula

determination. Thus, MS analysis was carried out on an electrospray hybrid quadrupole time-of flight mass spectrometer microTOF-Q (Bruker-Daltonik, Bremen, Germany) equipped with an electrospray ionization (ESI) ion source. Mass spectra for metabolite extracted samples were acquired both in positive and in negative ion mode. ESI capillary voltage was set at 4500V (+) (-) ion mode. The liquid nebulizer was set to 27 psi and the nitrogen drying gas was set to a flow rate of 6 L/min. Dry gas temperature was maintained at 200°C. Data were stored in centroid mode. Data were acquired with a stored mass range of m/z 50–1200. Automatic isolation and fragmentation (AutoMS^n mode) was performed on the 4 most intense ions simultaneously throughout the whole scanning period (30 min per run). Calibration of the mass analyzer is essential in order to maintain a high level of mass accuracy. Instrument calibration was performed externally every day with a sodium formate solution consisting of 10 mM sodium hydroxide in 50% isopropanol: water, 0.1 % formic acid. Automated internal mass scale calibration was performed through direct automated injection of the calibration solution at the beginning and at the end of each run by a 6-port divert-valve.

Targeted metabolobomics and lipidomics: Multiple Reaction Monitoring

Metabolites of interest were thus further tested for validation with multiple reaction monitoring (MRM), as previously reported[20]. Instrument set up, calibration curves and relative quantization were performed against external standards from Sigma. Each standard compound was weighted and dissolved in nanopure water. Starting at a concentration of 1 mg/ml of the original standard solution, a dilution series of steps (in 18 MO, 5% formic acid) was performed for each of the standards in order to reach the limit of detection (LOD) and limit of quantification (LOQ), as previously reported.[19,20] Metabolites were directly eluted into a High Capacity ion Trap HCTplus (Bruker-Daltonik). Mass spectra for metabolite extracted samples were acquired in positive ion mode, as previously described[19]. ESI capillary voltage was set at 3000 V (+) ion mode. The liquid nebulizer was set to 30 psi and the nitrogen drying gas was set to a flow rate of 9 L/min. Dry gas temperature was maintained at 300°C. Internal reference ions were used to continuously maintain mass accuracy. Data were acquired at the rate of 5 spectra/s with a stored mass range of m/z 50–1500. Data were collected using Bruker Esquire Control (v. 5.3 – build 11) data acquisition software. In MRM analysis, m/z of interest were isolated, fragmented and monitored (either the parental or fragment ions) throughout the whole RT range. Validation of HPLC online MS-eluted metabolites was performed by comparing transitions fingerprint, upon fragmentation and matching against the standards metabolites (Sigma) through direct infusion with a syringe pump (infusion rate

4 μl/min). Robustness and linearity of the method were confirmed to be in agreement with our previous reports.[19,20] Stability of oxidation-prone compounds, such as GSH, under the experimental conditions described above, was confirmed at 1h, 1day and 1 week from sample preparation (samples stored at -80°C).

Data elaboration and statistical analysis

Triplicate technical runs for biological replicates (n=5) for each group (non-ischemic control, ischemic, and ischemic retinas treated either with OCT, PACAP or SP) were exported as mzXML files and processed through MAVEN[34]. Mass spectrometry chromatograms were elaborated for peak alignment, matching and comparison of parent and fragment ions, and tentative metabolite identification (within a 20 ppm mass-deviation range between observed and expected results against the KEGG pathway database)[35]. In order to reduce the number of possible hits in molecular formula generation, we exploited the Compound Mass Formula application within the MAVEN software package (Princeton University, NJ, USA) and SmartFormula 3D (Bruker Daltonics, Bremen, Germany), which directly calculate molecular formulae based upon the MS spectrum (isotopic patterns) and transition fingerprints (MS/MS fragmentation patterns). This software generates a confidence-based list of chemical formulae on the basis of the precursor ions and all fragment ions, and the significance of their deviations to the predicted intact mass and fragmentation pattern (within a predefined window range of 5 ppm). Relative quantization and pathway representations were determined upon normalization against non-ischemic controls in a pathway-wise fashion. Statistical significance was determined at p-value < 0.05, 0.01 or 0.001 (ANOVA) upon comparison of treated groups to untreated control or ischemic retinas, through GraphPad Prism (GraphPad Software, San Diego, CA, USA).

Results and Discussion

Experimental model

In the present study, *ex vivo* retinal ischemia was induced by incubating the retinas in an oxygen-depleted solution containing 10^{-3} M sodium azide. Sodium azide inhibits mitochondrial complex IV by binding with molecular iron associated with cytochrome oxidase and prevents the production of ATP. It causes the generation of reactive oxygen species and induces caspase-3 production and apoptosis in neuronal cells[36]. As shown in **Fig. 1A-D**, no TUNEL labeling was observed in sections from non-ischemic control retinas or from retinas incubated in the ischemic solution for 30 minutes, while only very faint TUNEL signal was detected after 1 hour incubation. Significant TUNEL staining was present in the ONL, the INL and the GCL after 3 hour ischemic treatment (**Fig. 1E**). Compared to our previous ischemic model[5], the rate of apoptotic cell death was similar in the ONL (about 38% vs 35%) and lower in the INL (about 13% vs 20%) and in the GCL (about 19% vs 30%). Overall, the observed cell loss in the retinal layers was similar to that reported in an *ex vivo* model of the ischemic rat retina[12,37] or in *in vivo* models of ischemia-reperfusion injury[38-40].

Effects of OCT, PACAP or SP on apoptosis and vascular endothelial growth factor (VEGF) expression

The effects of OCT, PACAP or SP were evaluated in retinas incubated in ischemic solution for 3 hours. All the three tested treatments resulted in notable reduction of TUNEL staining in the ONL, the INL and the GCL (**Fig. 1F-G**). In particular, as shown in **Fig. 1I**, OCT almost prevented cell death in all nuclear retinal layers, while PACAP or SP reduced cell death of about 85% in the ONL, 75% in the INL, and 95% in the GCL. Consistent with our previous data[5,6] and with other studies in guinea pig and rat retinas[7,12,37], these observations show a potent protective effect of OCT against ischemia-induced apoptosis, as evaluated with TUNEL staining, thus confirming and expanding the notion that sst_2 receptor agonists possess a promising therapeutic potential to treat retinal pathologies[8,9,14]. Most importantly, our results show that additional peptidergic systems, namely PACAP and SP, display significant anti-apoptotic effects in the ischemic retina and they may contribute to the arsenal of retinal anti-ischemic drugs. If such an action could be expected for PACAP in view of its reported protective effects in the retina[15], this is the first demonstration, to our knowledge, of a protective role of SP in retinal ischemia.

The expression of caspase-3 mRNA was significantly increased in ischemic retinas with respect to non-ischemic controls, while treatments with OCT, PACAP or SP resulted in values of caspase-3

316 mRNA expression that were not significantly different from those detected in non-ischemic control
317 retinas (**Fig. 2A**). The observation that the expression of caspase-3 mRNA increases in the ischemic
318 retina confirms our previous results[5] and is consistent with data indicating that ischemia-induced
319 apoptosis in the retina is executed at least in part by caspase-3-dependent pathway[41]. Caspase-3 is a
320 key player in ischemia-induced apoptosis in response to various stimuli and, in particular,
321 downstream to glutamate excitotoxicity signaling pathways[42]. The effect of OCT, which abolishes
322 the ischemia-induced increase of caspase-3 mRNA, is in line with results obtained with retinas of
323 sst_1 receptor knockout mice, which over-express functional sst_2 receptors[5]. In addition, our results
324 demonstrating similar effects of PACAP and SP confirm that these peptides may exert important
325 anti-apoptotic actions in the ischemic retina.
326 Since an ischemic condition not only promotes cell death, but also induces vascular responses[3], we
327 evaluated this aspect by assessing VEGF mRNA levels following ischemic treatment. VEGF mRNA
328 levels were observed to dramatically increase in ischemic retinas, but this effect was abolished by
329 treatments with OCT, PACAP or SP (**Fig. 2B**). The finding of significantly increased VEGF mRNA
330 in the ischemic retina is in line with the stimulating effect of hypoxia on VEGF expression in
331 hypoxic retinas[43], however, it is in apparent contrast with our previous finding of reduced VEGF
332 mRNA in *ex vivo* mouse retinas treated for 1 hour with an ischemic solution containing iodoacetic
333 acid[10]. A likely explanation is that the 1 hour survival in extremely adverse ischemic conditions is
334 too short to activate transcription of VEGF mRNA at detectable levels, and only a massive release
335 of VEGF from neurons and an accumulation of VEGF in retinal vessels takes place in those
336 retinas[10]. In contrast, the survival of the retinas in the present study is 3 hours and the ischemic
337 conditions are less severe, thus allowing the activation of hypoxia-inducible factor and VEGF
338 upregulation. In other words, in the iodoacetic acid-treated retinas, neurons (which appear to be the
339 main sources of VEGF in the mouse retina[10]) are incapable of increasing VEGF expression since
340 they undergo fast and extensive apoptotic cell death[5]. In contrast, in sodium azide-treated retinas,
341 neurons display a longer survival time and a reduced percentage of cell death in the INL and in the
342 GCL, thus retaining the potential of increasing their VEGF expression. We demonstrate here that
343 the treatment of ischemic retinas with OCT, PACAP or SP counteracts the effects of ischemia and
344 reverts VEGF levels to those of non-ischemic retinas. This effect of OCT is consistent with the
345 results of studies in hypoxic retinal models[43]. Instead, PACAP has been reported to promote VEGF
346 expression in tumor cells, while SP has been observed to promote angiogenesis in different
347 experimental models (see Ribatti et al.[44], for review). Our hypothesis is that VEGF is released[10]

and possibly synthesized (present study) by retinal neurons when they start suffering from of oxygen and nutrient shortage and in the presence of increasing apoptotic molecules. If neurons are protected from metabolic stress and apoptosis, they would release and synthesize less VEGF; therefore factors with neuroprotective potential, such as OCT, PACAP or SP, would also limit the neuron-mediated VEGF increase in ischemic conditions.

Overview of the metabolomic analyses

Metabolomics results are plotted in **Figs. 3-10** as fold-change variations of metabolites, normalized to non-ischemic retinas, upon ischemia and OCT, PACAP or SP treatment. Metabolites were grouped following a pathway-based criterion, including: (i) glutamate accumulation and glutathione (GSH) homeostasis (**Figs. 3 and 4**); (ii) oxidized lipids and inflammatory mediators (**Suppl. Fig. 2**); (iii) arginine-citrulline-nitric oxide (NO) metabolism and signaling molecules (**Suppl. Fig. 3**); (iv) Pentose Phosphate Pathway (PPP) (**Fig. 5**); (v) glycolysis (**Fig. 6**); (vi) Krebs cycle (**Suppl. Fig. 4**); and (vii) purine metabolism (**Suppl. Fig. 5**).

Glutamate accumulation and alteration of GSH homeostasis

One of the distinct features of ischemia-induced neural injury is glutamate excitotoxicity[2]. In the present study, we observed significantly increased levels of glutamate following ischemic treatment (109.65 $\pm$ 1.64 fold-change increase in comparison to non-ischemic retinas), that were significantly decreased, albeit not fully restored back to normal values, by the exposure to OCT, PACAP, or SP (**Fig. 3A**). Of note, the ischemic treatment also significantly altered the levels of the glutamate precursor glutamine (**Fig. 3B**), a condition that was restored by all the assayed treatments. These effects of OCT confirm previous evidence demonstrating reduced glutamate release in ischemic retinas over-expressing functional sst_2 receptors[5] or in ischemic retinas treated with OCT[6]. In addition, these data are in line with observations of protective effects of PACAP or SP against excitotoxic insults[45,46], although direct effects of these peptides in the modulation of glutamate release have not been reported previously.

Since ischemia is associated with oxidative injury[2], we wondered whether GSH homeostasis was also altered by the ischemic treatment to some extent. Untargeted metabolomics results showed a positive effect of PACAP or SP on the accumulation of GSH, a phenomenon that was not induced by OCT (**Fig. 3C**). On the other hand, ischemia resulted in significant accumulation of oxidized glutathione (GSSG), a condition that was fully restored by OCT or SP and partially, albeit still

significantly, by PACAP (**Fig. 3D**). Increased levels of GSSG in the ischemic retina have been reported[47,48] and therapeutic interventions based on the administration of antioxidants have been proposed[48]. Consistent with these observations, we measured increased levels of the GSH precursor γ-glutamyl cysteine in ischemic conditions and reduction of these levels upon treatment with OCT, PACAP or SP (**Fig. 3E**). GSH is a tripeptide of glutamate, glycine and cysteine, the latter being a rate-limiting substrate for GSH biosynthesis. Ischemic injury was associated with decreased cysteine levels (**Fig. 3F**), which could result from increased cysteine consumption in response to the increased need for GSH, as suggested by the effect of OCT recorded with targeted metabolomic analyses (see **Fig. 4B**), and of PACAP and SP as suggested by untargeted metabolomics (see **Fig. 3C**).

Ischemic injury promoted the accumulation of L-homocysteine (**Fig. 3G**), a phenomenon that was not counteracted by PACAP or SP. On the other hand, OCT decreased L-homocysteine levels below those in non-ischemic retinas. This is relevant in the light of the documented association between the levels of homocysteine and adenosylhomocysteine and retinal microvascular abnormalities[49], although no effects of ischemia or of the peptide treatments were observed in the levels of adenosylhomocysteine (**Fig. 3H**).

In order to validate these results, we performed a targeted and orthogonal MRM metabolic analysis of the metabolites involved in GSH homeostasis (**Fig. 4**). As a result, we could confirm the evidence from untargeted metabolomics for glutamate and GSSG, while MRM analyses indicated a decrease (instead of no significant change) of the GSH levels upon ischemic treatment. Both targeted and untargeted approaches showed that OCT treatment produced GSH/GSSG ratios that were not significantly different from non-ischemic controls. Overall, these results suggest that PACAP and SP are capable of counteracting the ischemia-induced oxidative stress, while OCT might just prevent oxidative stress accumulation.

Peroxidized lipids and inflammatory mediators

We documented oxidative stress following ischemic injury at the lipid level, with the accumulation of pro-flogosis effectors, including prostaglandins (D2/E2, F1α), leukotrienes (C4), thromboxanes (A2) and oxysterols (cholest-5-ene-3-β,26-diol; 5,6-epoxy 18R-HEPE; 7α,24-dihydroxy-4-cholesten-3one) (**Suppl. Fig. 2A-D, F-H**). On the other hand, lipid turn-over was reduced upon ischemic injury, as deduced by the observed decrease of carnitine (**Suppl. Fig. 2E**), a trend that was significantly contrasted by the treatment with OCT or SP. These results are consistent with the

previously reported accumulation of oxidative stress targeting the lipid fraction in the ischemic retina[50], which is known to trigger pro-inflammatory responses that promote flogosis and local vasculature responses during reperfusion[51]. The accumulation of pro-inflammatory factors was reverted by OCT, PACAP or SP treatment. In particular, OCT relieved prostaglandin F1α accumulation better than PACAP or SP.

Nitric oxide (NO) metabolism

NO synthesis results from the conversion of L-arginine, in the presence of NADPH and oxygen, into NO and citrulline, catalyzed by the enzyme NO synthase. This enzyme competes with arginase for the substrate L-arginine[52], and deletion/demodulation of arginase reduces neuro-glial injury and improves neuronal function in a model of retinopathy of prematurity[53], suggesting that arginine availability for NO synthesis may result in protective effects. Arginine is one of the key intermediate metabolites of the citrulline-arginine-ornithine cycle in the urea cycle. These metabolites (arginine, ornithine, citrulline) were found to be up-regulated in ischemic retinas, while the treatment with OCT, PACAP or SP demodulated this effect (**Suppl. Fig. 3A-C**), with OCT promoting down-regulation of arginine, ornithine and citrulline to levels below the non-ischemic controls. These observations may indicate a role of OCT in directing arginine utilization towards NO production. In particular, arginine is converted into ornithine and urea by arginase, and then further transformed into citrulline in the urea cycle. On the other hand, arginine is also a substrate of NO synthase for the production of NO (a reaction that directly produces citrulline). In the present study, OCT-induced decrease of arginine was not paralleled by ornithine and citrulline accumulation. In general, increased consumption rates of metabolic intermediates (such as in this case) could result from over-activation of metabolic fluxes through a given pathway (though further labeling experiments are mandatory to draw any definitive conclusion). However, the present results suggest that the possibility exists that OCT treatment might promote NO production. This hypothesis will deserve further testing in the future, in the light of the reported increase in NO production induced by sst_2 receptor agonists[54], which is suggestive of a role for NO as a mediator of the neuroprotective effects of somatostatin in the ischemic retina[37].

cAMP, IP3 and PIP2/PIP3 ratio

Ischemic retinas showed significantly decreased levels of cAMP in comparison to non-ischemic controls (**Suppl. Fig. 3D**). This effect was restored by all treatments, with OCT appearing as less

efficacious than PACAP or SP. While correlations between the somatostatinergic system and adenylate cyclase have been previously reported in the literature[26], a key role in cAMP production was expected for PACAP (owing to its name reflecting its downstream activated pathways). Indeed, the neuroprotective effect of PACAP is predominantly mediated by PAC1 receptors, and it involves protein kinase A (PKA), cAMP response element binding, extracellular signal-regulated kinase phosphorylation, and the PKA/Bad/14-3-3 protein cascade resulting in increased expression of the protective Bcl-xL and Bcl-2[55]. Although SP signaling should not involve cAMP production, we could also detect control-like levels of cAMP in SP-treated ischemic retinas (**Suppl. Fig. 3D**). The possibility exists that SP counteracts the ischemia-induced cAMP reduction through indirect mechanisms not involving a direct action of SP on adenylate cyclase activity.

Alteration of calcium signaling in response to ischemia is one of the central events tied to glutamate release at the synaptic level[56]. Calcium reservoirs in the endoplasmic reticulum and mitochondria are indirectly regulated by signaling molecules, such as inositol triphosphate (IP3). In line with these considerations, ischemia induced upregulation of inositol. This effect was abolished by all treatments (**Suppl. Fig. 3E**), while upregulation of IP3 was relieved by OCT or SP (**Suppl. Fig. 3F**). Ischemia also induced the accumulation of the IP3 precursor phosphatidyl-inositol 4,5 phosphate (PIP2) (**Suppl. Fig. 3G**). This is relevant in the light of the role of PIP2 accumulation in triggering pro-apoptotic cascades, via shifting cellular signaling from the IP3 kinase (IP3K)-mediated accumulation of phosphatidyl-inositol 3,4,5-triphosphate (PIP3) and subsequent activation of Akt and Akt-regulated pro-survival pathways[57,58]. Since PIP3 promotes survival and PIP2 (indirectly) apoptosis, the PIP3/PIP2 ratio is inversely related to the triggering of pro-apoptotic cascades. Indeed, ischemia induced a two-fold increase of PIP3 and a four-fold increase of PIP2, which halved the PIP3/PIP2 ratio observed in non-ischemic controls (**Suppl. Fig. 3G and 3H**). While restoring PIP2 levels back to control values, PACAP treatment resulted in decreased levels of PIP3, which reduced the PIP3/PIP2 ratio in comparison to non-ischemic controls. Conversely, OCT in particular and, to a lesser extent, SP, restored PIP3/PIP2 ratios back to control values (**Suppl. Fig. 3G and 3H**). These results complement data available from the literature, whereby a role has been suggested for OCT, PACAP, and SP in modulating anti-apoptotic and anti-proliferative actions via IP3K/Akt pathways in pituitary tumor cells[59], human retinal pigment epithelial cells[60], and human mesenteric preadipocytes[61], respectively.

Metabolic shift towards the pentose phosphate pathway (PPP)

Ischemic retinas were generally characterized by higher levels of metabolites of the PPP, including early oxidative phase intermediates (glucose 6-phosphate, 6-phosphogluconolactone) and non-oxidative phase metabolites (ribulose 5-phosphate) (**Fig. 5**). Metabolic shifts towards the PPP are required during anabolism or in response to oxidative stress[62], to provide reducing coenzyme NADPH to restore GSH from GSSG and to replenish the antioxidant battery of several antioxidant enzymes (for example GSH peroxidase). In ischemic retinopathy, NADPH oxidase activity is tied to the overexpression of VEGF and induces neovascularization[64]. On the other hand, NADPH oxidase deletion promotes neuroprotection in retinal ischemia/reperfusion injury[64]. Notably, neither PACAP nor SP counteracted ischemia-induced metabolic diversion towards the PPP (**Fig. 5A-D**), suggesting that ischemic retinas treated with PACAP or SP still need to cope with oxidative stress. Indirectly, this emerges also from the observation of NADPH levels (**Fig. 5E**), which were increased only two-fold in ischemic retinas in comparison to non-ischemic controls, while higher NADPH levels were observed in OCT or PACAP-treated but not in SP-treated ischemic retinas. These data also suggest that OCT-treated ischemic retinas are less affected by oxidative stress and thus conserve higher reservoirs of NADPH, according with the observation that OCT-treated retinas seem not to suffer from the metabolic shift towards the PPP. On the other hand, PACAP seems to promote the shift towards PPP while maintaining higher levels of NADPH in comparison to SP-treated or untreated ischemic retinas, suggesting that PACAP might be more effective than SP in defending the retina from ischemia-induced oxidative stress. However, it is also worthwhile to note that build-up of metabolic intermediates of a certain pathway might either testify an over-activation of that specific pathway, or rather a blockade downstream to it (for example, at the non-oxidative phase of the PPP), which would result in late PPP intermediates (such as erythrose phosphate) being fluxed back to early oxidative phase ones or just being accumulated since they are less fluxed to other pathways. Therefore, in the absence of data from stable isotope labeling with [U-13$C_{1,2}$]-glucose and its derivatives, it is also worth considering that higher levels of erythrose 4-phosphate in OCT-treated ischemic retinas (**Fig. 5F**) can be either suggestive of an action of OCT towards (i) the deregulated utilization of erythrose phosphate in down-stream pathways or (ii) the promotion of metabolic fluxes from the non-oxidative PPP arm towards the main glycolytic pathway; finally, build-up of erythrose phosphate might also (iii) promote the biosynthesis of aromatic amino acids (tyrosine, phenylalanine and tryptophan), of which erythrose 4-phosphate serves as a co-substrate with phosphoenolpyruvate. However, we could not provide supporting evidence to none of these

hypotheses (energy metabolism is discussed in the following paragraph), especially as far as aromatic acids are concerned, since we could not observe any major alterations in the levels of tyrosine, tryptophan or phenylalanine in OCT-treated ischemic retinas (data not shown).

Energy metabolism and oxidative phosphorylation

As anticipated in the previous paragraphs, ischemic retinas are known to suffer from impaired energy metabolism (namely, depletion of ATP reservoirs), which promotes calcium dysregulation and glutamate release[2,56]. This is consistent with a reduced glycolytic rate through the Embden Meyerhof pathway (**Fig. 6**), resulting from a shift towards the PPP, as described above. In detail, except for glucose 6-phosphate (**Fig. 6A**), that has already been discussed in the previous paragraph since it also represents the first metabolite of the PPP, all glycolytic intermediates suffered from a significant decrease upon ischemic treatment (fructose 1,6-biphosphate, dihydroxyacetone phosphate, glyceraldehyde 3-phosphate (G3P), 2,3-diphosphoglycerate (DPG), phosphoglycerate; **Fig. 6B-F**), a trend that was challenged only in part by some of the treatments. In particular, only PACAP boosted the production of DPG (**Fig. 6E**) while PACAP and SP increased the levels of phosphoenolpyruvate (PEP– **Fig. 6G**) and OCT levels did not significantly vary in comparison to non-ischemic controls or ischemic retinas for these two metabolites. Although it is difficult to deduce any definitive explanation to these observations, a hypothesis is that any shift towards the PPP should drive metabolic fluxes to the purine biosynthesis pathway, to the aromatic acid biosynthesis, or rather re-enter glycolysis, though downstream to G3P. Several lines of evidence support the latter hypothesis, since both DPG and PEP are downstream to G3P, and both PACAP and SP, albeit not OCT, maintain the ischemia-induced shift towards the PPP. Conversely, it is interesting to note that despite apparently promoting the PPP, ischemia did not result in major deviations from the non-ischemic control in the levels of DPG and PEP, which is suggestive of a blockade at the non-oxidative phase level of PPP before re-entering the canonical glycolytic pathway.

Depletion of early glycolytic intermediates can also result from a more rapid fluxing towards the accumulation of end-products. Indeed, ischemia promoted the accumulation of lactate (**Fig. 6H**), which is particularly relevant when considering that glycolysis ensues under anaerobic conditions (and in this case, in response to anaerobiosis-mimetic ischemia). In addition, this effect was reverted by OCT, but not by PACAP or SP. In the absence of information about metabolic fluxes through stable isotope labeling, we may hypothesize that the observed consumption of early

glycolytic intermediates accompanied by lactate accumulation in response to ischemia might derive from an exacerbated glycolytic rate. Indeed, build-up of lactate represents a well-established signature of an exacerbated (anaerobic) glycolysis, which is relevant in that it fits with the observed ischemia-induced increased transcription of VEGF (**Fig. 2.B**), a marker often associated to hypoxic stress.[43] On the other hand, lactate accumulation might rather derive from the up-regulation of alternative pathways, such as the glyoxalase system, which is known to prevent retinal neuroglial and vasodegenerative pathologies through the conversion of oxoaldehydes, thus promoting the formation of dangerous advanced glycation end-products[65]. The final product of this antioxidant pathway is indeed lactate, passing through the lactoyl-glutathione intermediate[66], whose relative levels were increased in the ischemic retinas, and were returned to control values after treatment with OCT but not with PACAP or SP (**Fig. 6I**). It is also worthwhile to stress that the intertwinement between glycolysis and oxidative stress is not only limited to the shift towards the PPP and methylgyloxal (glyoxalase system), but it might also involve the direct scavenging of reactive nitrogen species by certain glycolytic intermediates[67].

A superficial interpretation of the results related to Krebs cycle intermediates might suggest that the oxidative arm of tricarboxylic acid cycle was apparently up-regulated in ischemic retinas (**Suppl. Fig. 4A-E**), especially downstream to α-ketoglutarate (**Fig. 9B**) at the level of succinyl-CoA and NADH (**Suppl. Fig. 4C and 4E**, respectively). In particular, α-ketoglutarate might enter the Krebs cycle as a direct metabolite of glutamate (by several enzymes, including glutamate dehydrogenase) upon its glutaminase-dependent conversion from glutamine, and downstream to citrate/isocitrate **Suppl. Fig. 4A**) which indeed were not apparently altered by ischemia. These effects were almost completely reverted by OCT (**Suppl. Fig. 4A-E**), while PACAP and SP seemed to exacerbate the ischemic effect on the Krebs cycle metabolism downstream to α-ketoglutarate (in particular for succinyl-CoA, succinate and NADH - **Suppl. Fig. 4C-E**). On the other hand, it can be argued that, in the absence of stable isotope labeling from glucose (or alternative carbon sources that might fuel the Krebs cycle – such as fatty acids or glutamine), it is difficult to conclude whether the observed ischemia-dependent accumulation of Krebs cycle intermediates α-ketoglutarate and succinyl-CoA might result from over-activation of the Krebs cycle or a blockade downstream to succinyl-CoA (succinate dehydrogenase, fumarase or malate dehydrogenase). A healthy Krebs cycle indeed results in the generation of glutamate and aspartate through the activity of glutamate-oxalacetate transaminases (GOT) from α-ketoglutarate and oxalacetate carbon sources, respectively. Glutamate generation might also result from the alanine-dependent transamination of α-ketoglutarate by

glutamate-pyruvate transaminase (GPT). In this view, increased levels of ischemic α-ketoglutarate might be consistent with the observed ischemia-dependent accumulation of glutamate and the decrease in ATP production (lower levels of ATP were detected in ischemic and treated retinas – **Suppl. Fig. 4F**). This might mean that ischemia uncouples fluxing through the Krebs cycle from ATP production, which could relate to the previously reported ischemia-dependent production of reactive oxygen species (ROS) at the mitochondria, mitochondrial apoptosis and impairment of the oxidative phosphorylation following ischemia[68] and is consistent with the hereby documented caspase-3 upregulation. It is however worth noting that, although ATP levels remained lower than in non-ischemic controls, OCT, PACAP or SP partly replenished ATP reservoirs (**Suppl. Fig. 4F**).

Purine metabolism

In prolonged ischemia, the breakdown products of ATP metabolism accumulate, including adenine, adenosine, hypoxanthine and inosine[69-71]. Adenosine is thought to provide protective effects during ischemia by targeting adenosine A1 receptor[70], whereas overstimulation of the A2a receptors has deleterious effects[69]. On the other hand, prolonged accumulation of adenosine may serve as a substrate for the formation of ROS[69,71]. Besides, prolonged ischemia results in increased production of xanthine, also promoting ROS formation through the activity of xanthine oxidase on hypoxanthine, thus exacerbating the ischemic damage to the retina[70,71]. Also, hypoxanthine might be produced from deamination of adenine, a process involved in the ischemic injury to guinea pig hearts[73]. Consistent with these data, our results show that ischemia promoted the accumulation of purine catabolites (adenine, adenosine, hypoxanthine, inosine – **Suppl. Fig. 5A, 5B, 5C and 5D**, respectively). In addition, these effects were further favored by PACAP or SP treatment. Conversely, OCT treatment resulted in significant decrease of the ischemia-induced levels of purine catabolites. No effects of ischemia were observed concerning the AMP levels (**Suppl. Fig. 5E**), while those of inosine monophosphate resulted increased by ischemia and reverted at or near control values by OCT, PACAP or SP (**Suppl. Fig. 5F**).

Conclusion

In summary, based on a recently optimized *ex vivo* model for retinal ischemia, we could monitor the major changes occurring at the metabolic level in response to treatments with OCT, PACAP, or SP. All the treatments decreased cell death and down-regulated VEGF mRNA levels, demonstrating that, in addition to that of somatostatin, at least two other peptidergic systems, namely PACAP and SP, deserve attention in view of peptide-based therapies to treat ischemic retinal disorders. The mass spectrometry-based metabolomic analysis evidenced that ischemia induces glutamate accumulation and alteration of GSH homeostasis, which are significantly restored back to normal by all the treatments. In particular, OCT seems to prevent the oxidative stress associated to ischemia, while PACAP or SP-treated retinas appear to actively cope with it. In addition, our observations revealed OCT, and to a lesser extent also PACAP and SP-mediated (i) a decreased accumulation of glutamate and normalization of glutathione homeostasis; (ii) a reduced build-up of α-ketoglutarate, that might serve as a substrate for the enhanced biosynthesis of glutamate in response to ischemia; (iii) a reduced accumulation of peroxidized lipids and inflammatory mediators; (iv) the normalization of glycolytic fluxes and thus prevented the over-accumulation of lactate, or either promoted the down-regulation of the glyoxalate anti-oxidant system; (v) a reduced metabolic shift from glycolysis towards the PPP or either a blockade at the non-oxidative phase of the PPP; (vi) tuning down of purine metabolism. In addition, OCT seems to be involved in NO production, although further investigations are needed to clarify this point. On the other hand, PACAP or SP-treated ischemic retinas show some distinct features, with the most significant being the up-regulation of the GSH anti-oxidant system. OCT, PACAP and SP are likely to modulate pro-survival signaling by restoring cAMP levels, IP3 signaling and PIP2/PIP3 ratios. None of the treatments was able to restore proper energy metabolism and ATP production, although ATP reservoirs were partly replenished by OCT, PACAP or SP.

To our knowledge, this is the first study to examine perturbations in the metabolome in relation to retinal ischemia and appropriate neuropeptide targets. The interactions of neuropeptides with metabolic network abnormalities, as demonstrated in the present study, open new perspectives in the discovery and development of peptide therapeutics against ischemia-induced retinal neuronal damage.

Acknowledgments

We thank Dr. Massimo dal Monte (Department of Biology, University of Pisa) for critical reading of the manuscript and Dr. Cristiano Papeschi (Bioetic Committee of the University of Tuscia) for animal care. This research was supported by fundings from the Italian Ministry of Education, by funds from the Italian National Blood Centre to ADA and LZ, and by mobility studentship and post-doctoral funds by the Interuniversity Consortium for Biotechnology to ADA.

Figure legends

Fig. 1. Summary of TUNEL staining in non-ischemic control and ischemic retinas, either untreated or treated with OCT, PACAP or SP or. (A) DAPI staining of a retinal section to show the retinal layers. (B) TUNEL staining in a non-ischemic control retina. (C, D, E) TUNEL staining in retinas treated with 10^{-3}M sodium azide for 30 min, 1 hour and 3 hours, respectively. (F, G, H) TUNEL staining in retinas treated with 10^{-3}M sodium azide for 3 hours plus OCT, PACAP or SP, respectively. Scale bar, 20 μm. (I) Quantitative analysis of the TUNEL staining in the outer nuclear layer (ONL), inner nuclear layer (INL) and ganglion cell layer (GCL). IPL, inner plexiform layer; OPL, outer plexiform layer. $^{§§}P < 0.01$; $^{§§§}P < 0.001$ against non-ischemic controls; *P <0.05; **P < 0.01; ***P < 0.001 against untreated ischemic retinas, ANOVA.

Fig. 2. qPCR of mRNAs encoding for caspase-3 (A) and VEGF (B) in ischemic retinas treated with OCT, PACAP or SP. Values are expressed as mean ± SEM (n = 5) of the fold change over non-ischemic retinas (broken line). $^{§§§}P < 0.0001$ against non-ischemic controls; **P < 0.001; ***P < 0.0001 against untreated ischemic retinas, ANOVA.

Fig. 3. GSH homeostasis and glutamate metabolism as assessed using untargeted metabolomic analyses. Values are expressed as mean ± SEM (n = 5) of the fold change over non-ischemic retinas (broken lines). $^{§}P < 0.01$; $^{§§}P < 0.001$; $^{§§§}P < 0.0001$ against non-ischemic controls; *P <0.01; **P < 0.001; ***P < 0.0001 against untreated ischemic retinas, ANOVA.

Fig. 4. Glutamate, GSH and GSSG levels detected through MRM targeted metabolomics. Values are expressed as mean ± SEM (n = 5) of the fold change over non-ischemic retinas (broken lines). $^{§§§}P < 0.0001$ against non-ischemic controls; *P <0.01; ***P < 0.0001 against untreated ischemic retinas, ANOVA.

Fig. 5. PPP related metabolites, as assessed using untargeted metabolomic analyses. Values are expressed as mean ± SEM (n = 5) of the fold change over non-ischemic retinas (broken lines). $^{§}P < 0.01$; $^{§§§}P < 0.0001$ against non-ischemic controls; *P <0.01; **P < 0.001; ***P < 0.0001 against untreated ischemic retinas, ANOVA.

669

670 **Fig. 6.** Glycolytic metabolism through the Embden Meyerhof pathway, as assessed using untargeted
671 metabolomic analyses. Values are expressed as mean ± SEM (n = 5) of the fold change over non-
672 ischemic retinas (broken lines). $^{\S}P < 0.01$; $^{\S\S\S}P < 0.0001$ against non-ischemic controls; *P <0.01;
673 **P < 0.001; ***P < 0.0001 against untreated ischemic retinas, ANOVA.

674

675

676 **Suppl. Fig. 1.** Representative gel electrophoresis of qPCR products.

677

678 **Suppl. Fig. 2.** Lipid peroxidation and pro-inflammatory markers, as assessed using untargeted
679 metabolomic analyses. Values are expressed as mean ± SEM (n = 5) of the fold change over non-
680 ischemic retinas (broken lines). $^{\S}P < 0.01$; $^{\S\S}P < 0.001$; $^{\S\S\S}P < 0.0001$ against non-ischemic controls;
681 *P <0.01; **P < 0.001; ***P < 0.0001 against untreated ischemic retinas, ANOVA.

682

683 **Suppl. Fig. 3.** Arginine-citrulline-ornithine nitric oxide-related metabolism and secondary
684 messenger metabolites (including cyclic AMP, inositol triphosphate, PIP2 and PIP3), as assessed
685 using untargeted metabolomic analyses. Values are expressed as mean ± SEM (n = 5) of the fold
686 change over non-ischemic retinas (broken lines). $^{\S}P < 0.01$; $^{\S\S\S}P < 0.0001$ against non-ischemic
687 controls; *P <0.01; **P < 0.001; ***P < 0.0001 against untreated ischemic retinas, ANOVA.

688

689 **Suppl. Fig. 4.** Krebs cycle metabolites, as assessed using untargeted metabolomic analyses. Values
690 are expressed as mean ± SEM (n = 5) of the fold change over non-ischemic retinas (broken lines).
691 $^{\S}P < 0.01$; $^{\S\S\S}P < 0.0001$ against non-ischemic controls; *P <0.01; **P < 0.001; ***P < 0.0001
692 against untreated ischemic retinas, ANOVA.

693

694 **Suppl. Fig. 5.** Purine metabolism, as assessed using untargeted metabolomic analyses. Values are
695 expressed as mean ± SEM (n = 5) of the fold change over non-ischemic retinas (broken lines). $^{\S}P <$
696 0.01; $^{\S\S\S}P < 0.0001$ against non-ischemic controls; *P <0.01; ***P < 0.0001 against untreated
697 ischemic retinas, ANOVA.

698

699

700

References

1. G. Minhas, R. Morishita, A. Anand, Preclinical models to investigate retinal ischemia: advances and drawbacks. *Front Neurol.* 2012, **3,** 75.
2. N.N. Osborne, R.J. Casson, J.P. Wood, G. Chidlow, M. Graham, J. Melena, Retinal ischemia: mechanisms of damage and potential therapeutic strategies. *Progr. Retinal Eye Res*., 2004, **23,** 91-147.
3. M. Rajappa, P. Sexena, J. Kaur, Ocular angiogenesis: mechanisms and recent advances in therapy. *Adv Clin Chem.*, 2010, **50,** 103-121.
4. P. Sapieha, D. Hamel, Z. Shao, J.C. Rivera, K. Zaniolo, J.S. Joyal, S. Chemtob, Proliferative retinopathies: angiogenesis that blinds, *Int. J. Biochem. Cell Biol*., 2010, **42(1)**, 5-12.
5. E. Catalani, D. Cervia, D. Martini, P. Bagnoli, E. Simonetti, A.M. Timperio, G. Casini, Changes in neuronal response to ischemia in retinas with genetic alterations of somatostatin receptor expression, *Eur. J. Neurosci.*, 2007, **25**, 1447-1459.
6. D. Cervia, D. Martini, C. Ristori, E. Catalani, A.M. Timperio, P. Bagnoli, G. Casini, Modulation of the neuronal response to ischaemia by somatostatin analogues in wild-type and knock-out mouse retinas, *J. Neurochem.,* 2008, **106**, 2224-2235.
7. U. Celiker, N. Ilhan, I. Ozercan, T. Demir, H. Celiker, Octreotide reduces ischaemia-reperfusion injury in the retina, *Acta Ophthalmologica Scandinavica*., 2002, **80**, 395-400.
8. D. Cervia, G. Casini, The Neuropeptide Systems and their Potential Role in the Treatment of Mammalian Retinal Ischemia: A Developing Story. Curr Neuropharmacol, *Curr Neuropharmacol*., 2013, **11**, 95-101.
9. D. Cervia, G. Casini, P. Bagnoli, Physiology and pathology of somatostatin in the mammalian retina: a current view, *Mol Cell Endocrinol*., 2008, **286**, 112-122.
10. D. Cervia, E. Catalani, M. Dal Monte, G. Casini, Vascular endothelial growth factor in the ischemic retina and its regulation by somatostatin, *J. Neurochem*., 2012, 120, 818-829.
11. D. Kokona, I. Mastrodimou, I. Pediaditakis, H. Charalampopoulos, A. Schmid, K. ThermosPasireotide, (SOM230) protects the retina in animal models of ischemia induced retinopathies. *Experimental Eye Research*., 2012, **103,** 90-98.
12. N. Mastrodimou, G.N. Lambrou, K. Thermos, Effect of somatostatin analogues on chemically induced ischaemia in the rat retina. *Naunyn Schmiedebergs Archivies of Pharmacol.,* 2005, **371,** 44-53.
13. P. McGonigle, Peptide therapeutics for CNS indications, *Biocheical Pharmacology*., 2012, **83,** 559-656.
14. D. Cervia, G. Casini, Recent advances in cellular and molecular aspects of mammalian retinal ischemia, *World J. Pharmacol.*, 2012, **1**, 30-43.
15. T. Nakamachi, A. Matkovits, T. Seki, S. Shioda, Distribution and protective function of pituitary adenylate cyclase-activating polypeptide in the retina, *Front. Endocrinol. (Lausanne)*., 2012, **3,** 145.
16. G. Bruno, F. Tega, A. Bruno, U. Graf, F. Corelli, R. Molfetta, M. Barucco, The role of substance P in cerebral ischemia, *Int. J. Immunopathol. Pharmacol.*, 2003, **16**, 67-72.
17. J.H. Yang, X.X. Meng, L.S. Xie, Z. Guo, Acute myocardial ischemia up-regulates substance P in the retina of rats. *Neurosci. Lett.*, 2008, **443,** 218-222.
18. G.J. Patti, O. Yanes, G. Siuzdak, Innovation: Metabolomics: the apogee of the omics trilogy. *Nature Rev. Mol. Cell. Biol*., 2012, **13,** 263-269.
19. A. D'Alessandro, F. Gevi, L. Zolla, A robust high resolution reversed-phase HPLC strategy to investigate various metabolic species in different biological models. *Mol Biosystem,* 2011, *7*, 1024-1032.
20. A. D'Alessandro, F. Gevi, L. Zolla, Targeted mass spectrometry-based metabolomic profiling through multiple reaction monitoring of liver and other biological matrices. *Meth. Mol. Biol., 2012,* **909**, 279-294.
21. A. D'Alessandro, G.M. D'Amici, S. Vaglio, L. Zolla, Time-course investigation of SAGM-stored leukocyte-filtered red bood cell concentrates: from metabolism to proteomics, *Haematologica*, 2012, **97**, 107-115.
22. F. Gevi, A. D'Alessandro, L. Zolla, Alterations of red blood cell metabolome during cold liquid storage of erythrocyte concentrates in CPD-SAGM, *J Proteomics*., 2012, **76,** 168-180.
23. R. Polati, A. Castagna, A.M. Bossi, Murine macrophages response to iron. *J. Proteomics.,* 2012, **76,** 10-27.
24. D. Cervia, C. Nunn, P. Bagnoli, Multiple signalling transduction mechanisms differentially coupled to somatostatin receptor subtypes: a current view, *Curr Enzyme Inhibition*., 2005, **1**, 265-279.
25. A. Bigiani, C. Petrucci, V. Ghiaroni, M. Dal Monte, A. Cozzi, H.J. Kreienkamp, D. Richter, P. Bagnoli, Functional correlates of somatostatin receptor 2 overexpression in the retina of mice with genetic deletion of somatostatin receptor 1, *Brain Res.,* 2004, **1025**, 177-185.
26. B. Pavan, S. Fiorini, M. Dal Monte, L. Lunghi, C. Biondi, P. Bagnoli, D. Cervia, Somatostatin coupling to adenylyl cyclase activity in the mouse retina. *Naunyn Schmiedebergs Arch. Pharmacol.,* 2004, **370,** 91-98.
27. T. Hamada, S. Shibata, The role of GABAergic neuron on NMDA- and SP-induced phase delays in the suprachiasmatic nucleus neuronal activity rhythm in vitro, *Neurosci Lett*., 2010, **468,** 344-347.

28. M. Kouznetsova, A. Nistri, Modulation by substance P of synaptic transmission in the mouse hippocampal slice. *Eur. J. Neurosci*., 1998, **10,** 3076-3084.
29. F. Pena, J.M. Ramirez, Substance P-mediated modulation of pacemaker properties in the mammalian respiratory network. *J Neurosci*., 2004, **24,** 7549-7556.
30. K. Shoge, H.K. Mishima, T. Saitoh, K. Ishihara, Y. Tamura, H. Shiomi, M. Sasa, Attenuation by PACAP of glutamate-induced neurotoxicity in cultured retinal neurons. *Brain Res*., 1999, **839,** 66-73.
31. M.S. Silveira, M. R. Costa, M. Bozza, R. Linden, Pituitary adenylyl cyclase-activating polypeptide prevents induced cell death in retinal tissue through activation of cyclic AMP-dependent protein kinase. *J. Biol. Chem*., 2002, **277,** 16075-16080.
32. K.J. Livak, T.D. Schmittgen, Analysis of relative gene expression data using real-time quantitative PCR and the 2(-Delta Delta C(T)) Method. *Methods*., 2001, **25,** 402-408.
33. A. D'Alessandro, F. Gevi, L. Zolla, Red blood cell metabolism under prolonged anaerobic storage, *Mol Biosyst.*, 2013, **9(6)**, 1196-1209.
34. E. Melamud, L. Vastag, J.D. Rabinowitz, Metabolomic analysis and visualization engine for LC-MS data. *Anal. Chem.*, 2011, **82,** 9818-9826.
35. M. Kanehisa, S. Goto, KEGG: kyoto encyclopedia of genes and genomes, *Nucleic Acids Res*., 2000, **28,** 27-30.
36. D. Ji, T.A. Kamalden, S. Olmo-Aguado, N.N. Osborne, Light- and sodium azide-induced death of RGC-5 cells in culture occurs via different mechanisms. *Apoptosis*, 2011, **16,** 425-437.
37. N. Mastrodimou, F. Kiagiadaki, K. Thermos, The role of nitric oxide and cGMP in somatostatin's protection against retinal ischemia. *Investigative Ophthalmol Vision Sci*., 2008, **49,** 342-349.
38. F. Dijk, W. Kamphuis, An immunocytochemical study on specific amacrine cell subpopulations in the rat retina after ischemia, *Brain Res,* 2004, **1026**, 205-317.
39. W.K. Ju, K.Y. Kim, Measuring glutamate receptor activation-induced apoptotic cell death in ischemic rat retina using the TUNEL assay, *Meth. Mol. Biol*., 2011, **740,** 149-156.
40. O. Oz, G. Gürelik, N. Akyürek, L. Cinel, A. Hondur, A short duration transient ischemia induces apoptosis in retinal layers: an experimental study in rabbits, *Europ. J. Ophthalmol.,* 2005, **15,** 233-238.
41. N. Katai, N. Yoshimura, Apoptotic retinal neuronal death by ischemia-reperfusion is executed by two distinct caspase family proteases. *Invest Ophthalmol Vis Science*., 1999, **40,** 2697-2705.
42. L. Tenneti, S.A. Lipton, Involvement of activated caspase-3-like proteases in N-methyl-D-aspartate-induced apoptosis in cerebrocortical neurons, *J. Neurochem*., 2000, **74,** 134-142.
43. S. Mei, M. Cammalleri, D. Azara, G. Casini, P. Bagnoli, M. Del Monte, Mechanisms underlying somatostatin receptor 2 down-regulation of vascular endothelial growth factor expression in response to hypoxia in mouse retinal explants. *J. Pathol*., 2012, **226,** 519-533.
44. D. Ribatti, M.T. Conconi, G.G. Nussdorfer, Nonclassic endogenous novel regulators of angiogenesis, *Pharmacolo. Rev*., 2007, **59,** 185-205.
45. N. Calvo, J. Reiriz, E. Pérez-Navarro, J. Alberch, Tachykinins protect cholinergic neurons from quinolinic acid excitotoxicity in striatal cultures, *Brain Res.,* 1996, **740**, 323-328.
46. K. Endo, T. Nakamachi, T. Seki, N. Kagami, Y. Wada, K. Nakamura, K. Kishimoto, M. Hori, D. Tsuchikawa, N. Shinntani, H. Hashimoto, A. Baba, R. Koide, S. Shioda, Neuroprotective effect of PACAP against NMDA-induced retinal damage in the mouse. *J. Mol. Neurosci.,* 2011, **43**, 22-29.
47. N. Dilsiz, A. Sahaboglu, M.Z. Yildiz, A. Reichenbach, Protective effects of various antioxidants during ischemia-reperfusion in the rat retina. *Graefes Arch. Clin. Exp.Ophthalmol.,* 2006, **244**, 627-633.
48. Z. Zhang, X. Qin, X. Zhao, N. Tong, Y. Gong, W. Zhang, X. Wu, Valproic acid regulates antioxidant enzymes and prevents ischemia/reperfusion injury in the rat retina, *Curr. Eye Res*., 2012, **37,** 429-437.
49. M.V. Van Hecke, J.M. Dekker, G. Nijpels, T. Teerlink, C. Jakobs, R.P. Stolk, R.J. Heine, L.M. Bouter, B.C. Polak, C.D. Stehouwer, Homocysteine, S-adenosylmethionine and S-adenosylhomocysteine are associated with retinal microvascular abnormalities: the Hoorn Study*, Clin. Sci.* (Lond)., 2008, **114,** 479-487.
50. S.Y. Li, Z.J. Fu, A.C. Lo, Hypoxia-induced oxidative stress in ischemic retinopathy. *Oxidative Medicine and Cellular Longevity.,* 2012**,** 426769.
51. S. Cuzzocrea, D.P. Riley, A. Caputi, D. Salvemini, Antioxidant therapy: a new pharmacological approach in shock, inflammation, and ischemia/reperfusion injury, *Pharmacol Revision., 2001,* **53**, 135-159.
52. W. Durante, F.K. Johnson, R.A. Johnson, Arginase: a critical regulator of nitric oxide synthesis and vascular function. *Clin. Exp. Pharmacol. Physiol., 2007,* **34**, 906-911.
53. S.P. Narayanan, J. Suwanpradid, A. Saul, Z. Xu, A. Still, R.W. Caldwell, R.B. Caldwell, Arginase 2 deletion reduces neuro-glial injury and improves retinal function in a model of retinopathy of prematurity *PLoS One*., 2011, **6,** e22460.
54. A. Vasilaki, M. Mouratidou, S. Schulz, K. Thermos, Somatostatin mediates nitric oxide production by activating sst(2) receptors in the rat retina, *Neuropharmacol.,* 2002, **43,** 899-909.

55. K. Szabadfi, L. Mester, D. Reglodi, P. Kiss, N. Babai, B. Racz, K. Kovacs, A. Szabo, A. Tamas, R. Gabriel, T. Atlasz, Novel neuroprotective strategies in ischemic retinal lesions. *Int. J. Mol. Sci*., 2010, **11,** 544-561.
56. H. Kuriyama, M. Nakagawa, M. Tsuda, Intracellular Ca(2+) changes induced by in vitro ischemia in rat retinal slices. *Exp. Eye Res*. 2001, **73,** 365-374.
57. C.H. Park, Y.S. Kim, Y.H. Kim, M.Y. Choi, J.M. Yoo, S.S. Kang, W.S. Choi, G.J. Cho, Calcineurin mediates AKT dephosphorylation in the ischemic rat retina. *Brain Research*., 2008, **1234,** 148-157.
58. S. Roth, A.R. Shaikh, M.M. Hennelly, Q. Li, V. Bindokas, C.E. Graham, Mitogen-activated protein kinases and retinal ischemia. *Invest. Ophthalmol. Vis. Sci.,* 2003, **44,** 5383-5395.
59. M. Theodoropoulou, J. Zhang, S. Laupheimer, M. Paez-Pereda, C. Erneux, T. Florio, U. Pagotto, G.K. Stalla, Octreotide, a somatostatin analogue, mediates its antiproliferative action in pituitary tumor cells by altering phosphatidylinositol 3-kinase signaling and inducing Zac1 expression, *Cancer Res*., 2006, **66,** 1576-1582.
60. E. Fabian, D. Reglodi, L. Mester, A. Szabo, K. Szabadfi, A. Tamas, G. Toth, K. Kovacs, Effects of PACAP on intracellular signaling pathways in human retinal pigment epithelial cells exposed to oxidative stress, *J. Mol. Neurosci*., 2012, **48**, 493-500.
61. K. Gross, I. Karagiannides, T. Thomou, H.W. Koon, C. Bowe, H. Kim, N. Giorgadze, T. Tchkonia, T. Pirtskhalava, J.L. Kirkland, C. Pothoulakis, Substance P promotes expansion of human mesenteric preadipocytes through proliferative and antiapoptotic pathways. *Am. J. Physiol. Gastrointestinal Liver Physiol.*., 2009, **296,** G1012-1019.
62. B.S. Winkler, M.J. Arnold, M.A. Brassell, D.R. Sliter, Glucose dependence of glycolysis, hexose monophosphate shunt activity, energy status, and the polyol pathway in retinas isolated from normal (nondiabetic) rats. *Invest. Ophthalmol. Vis. Sci.,* 1997, **38,** 62-71.
63. M. Al-Shabrawey, M. Bartoli, A.B. El-Remessy, D.H. Platt, S. Matragoon, M.A. Behzadian, R.W. Caldwell, R.B. Caldwell, Inhibition of NAD(P)H oxidase activity blocks vascular endothelial growth factor overexpression and neovascularization during ischemic retinopathy, *Am J Pathol*, 2005, **167**, 599-607.
64. H. Yokota, S.P. Narayanan, W. Zhang, H. Liu, M. Rojas, Z. Xu, T. Lemtalsi, T. Nagaoka, A. Yoshida, S.E. Brooks, R.W. Caldwell, R.B. Caldwell, Neuroprotection from retinal ischemia/reperfusion injury by NOX2 NADPH oxidase deletion, *Invest. Ophthalmol. Vis. Sci*., 2011, **52,** 8123-8131.
65. A.K. Berner, O. Brouwers, R. Pringle, I. Klaassen, L. Colhoun, C. McVicar, S. Brockbank, J.W. Curry, T. Miyata, M. Brownlee, R.O. Schlingemann, C. Schalkwijk, A.W. Stitt, Protection against methylglyoxal-derived AGEs by regulation of glyoxalase 1 prevents retinal neuroglial and vasodegenerative pathology, *Diabetologia.* 2012, **55**, 845-854.
66. B. Mannervik, Molecular enzymology of the glyoxalase system, *Drug Metabol Drug Interact*., 2008, **23,** 13-27.
67. J. Frenzel, J. Richter, K. J. Eschrich, Pyruvate protects glucose-deprived Muller cells from nitric oxide-induced oxidative stress by radical scavenging, *Glia*, 2005, **52,** 276-288.
68. H. Honda, P. Korge, J.N. Weiss, Mitochondria and ischemia/reperfusion injury. *Ann. New York Acad. Sci.,* 2005, **1047,** 248-258.
69. G.J. Ghiardi, J. M. Gidday, S. Roth, The purine nucleoside adenosine in retinal ischemia-reperfusion injury. *Vision Res*., 1999, **39,** 2519-2535.
70. S. Roth, S.S. Park, C.W. Sikorski, J. Osinski, R. Chan, K. Loomiset, Concentrations of adenosine and its metabolites in the rat retina/choroid during reperfusion after ischemia, *Curr. Eye Res.,* 1997, **16,** 875-885.
71. Roth, S., Rosenbaum, P.S., Osinski, J., Park SS, Toledano AY, Li B, Moshfeghi AA, Ischemia induces significant changes in purine nucleoside concentration in the retina-choroid in rats. *Exp. Eye Res.*, 1997, **65,** 771-779.
72. G.S. Sandhu, A.C. Burrier, D.R. Janero, Adenosine deaminase inhibitors attenuate ischemic injury and preserve energy balance in isolated guinea pig heart, *Am. J. Physiol.,* 1993, **265,** H1249-H1256.
73. P. Seeeha, D. Hamel, Z. Shao, Proliferative retinopathies: angiogenesis that blinds. *Int. J. Biochem. Cell Biol.*, 2010, **42,** 5-12.

Table 1. Primer pairs designed for qPCR analysis

*http://medgen.ugent.be/rtprimerdb/index.php

Name	Symbol	Gene accession N°	Primer sequence	Amplicon	Source
Caspase 3	*casp3*	NM_009810	F: 5'-GCACTGGAATGTCATCTCGCT-3' R: 5'-GGCCCATGAATGTCTCTCTGAG-3'	69 bp [nt 143-241]	PrimerBank#
VEGF	*vegfa*	NM_009505	F: 5'-GCACATAGAGAGAATGAGCTTCC-3' R: 5'-CTCCGCTCTGAACAAGGCT-3'	105 bp [nt 342-446]	PrimerBank#
GAPDH	*gapdh*	NM_008084	F: 5'-ACCCAGAAGACTGTGGATGG-3' R: 5'-ACACATTGGGGGTAGGAACA-3'	172 bp [nt 594-765]	RTPrimerDB*

#http://pga.mgh.harvard.edu/primerbank/

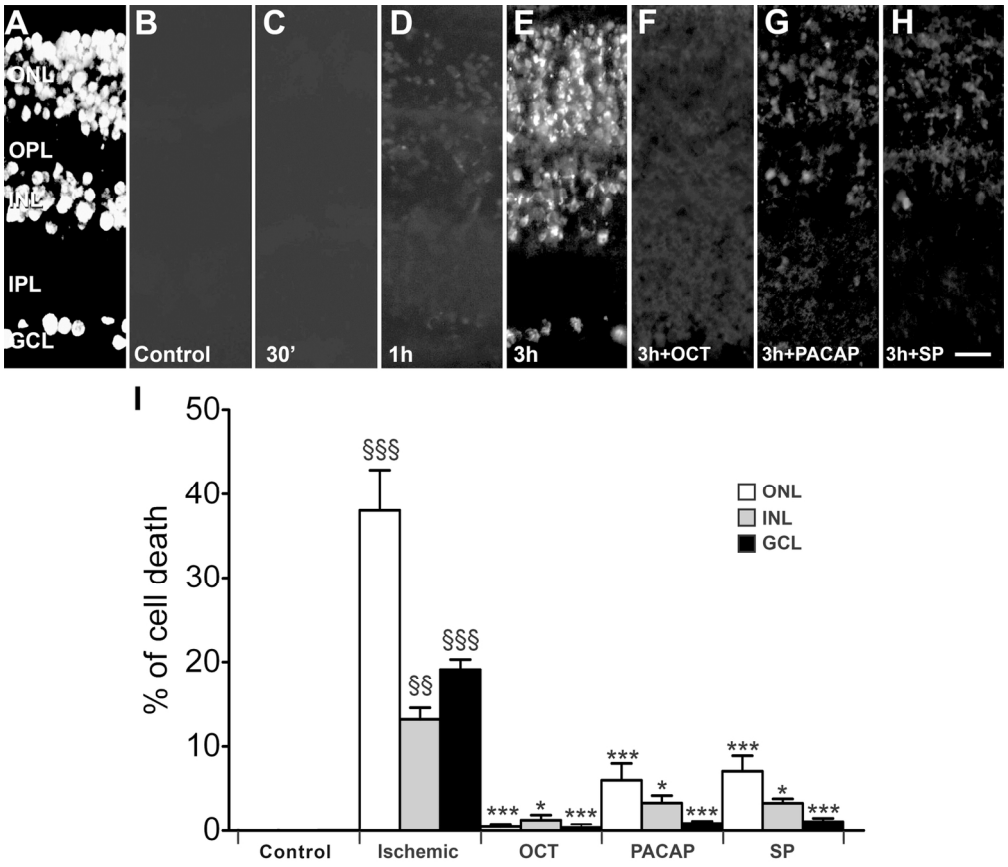

Fig. 1. Summary of TUNEL staining in non-ischemic control and ischemic retinas, either untreated or treated with OCT, PACAP or SP or. (A) DAPI staining of a retinal section to show the retinal layers. (B) TUNEL staining in a non-ischemic control retina. (C, D, E) TUNEL staining in retinas treated with 10-3M sodium azide for 30 min, 1 hour and 3 hours, respectively. (F, G, H) TUNEL staining in retinas treated with 10-3M sodium azide for 3 hours plus OCT, PACAP or SP, respectively. Scale bar, 20 μm. (I) Quantitative analysis of the TUNEL staining in the outer nuclear layer (ONL), inner nuclear layer (INL) and ganglion cell layer (GCL). IPL, inner plexiform layer; OPL, outer plexiform layer. §§P < 0.01; §§§P < 0.001 against non-ischemic controls; *P <0.05; **P < 0.01; ***P < 0.001 against untreated ischemic retinas, ANOVA.
147x127mm (300 x 300 DPI)

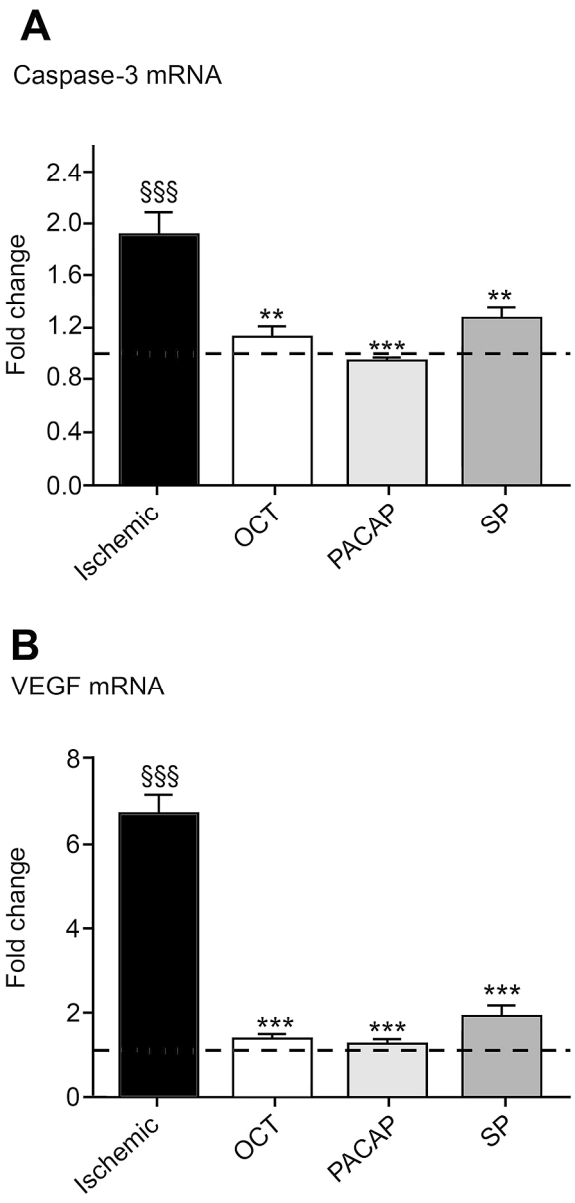

Fig. 2. qPCR of mRNAs encoding for caspase-3 (A) and VEGF (B) in ischemic retinas treated with OCT, PACAP or SP. Values are expressed as mean ± SEM (n = 5) of the fold change over non-ischemic retinas (broken line). §§§P < 0.0001 against non-ischemic controls; **P < 0.001; ***P < 0.0001 against untreated ischemic retinas, ANOVA.
180x363mm (600 x 600 DPI)

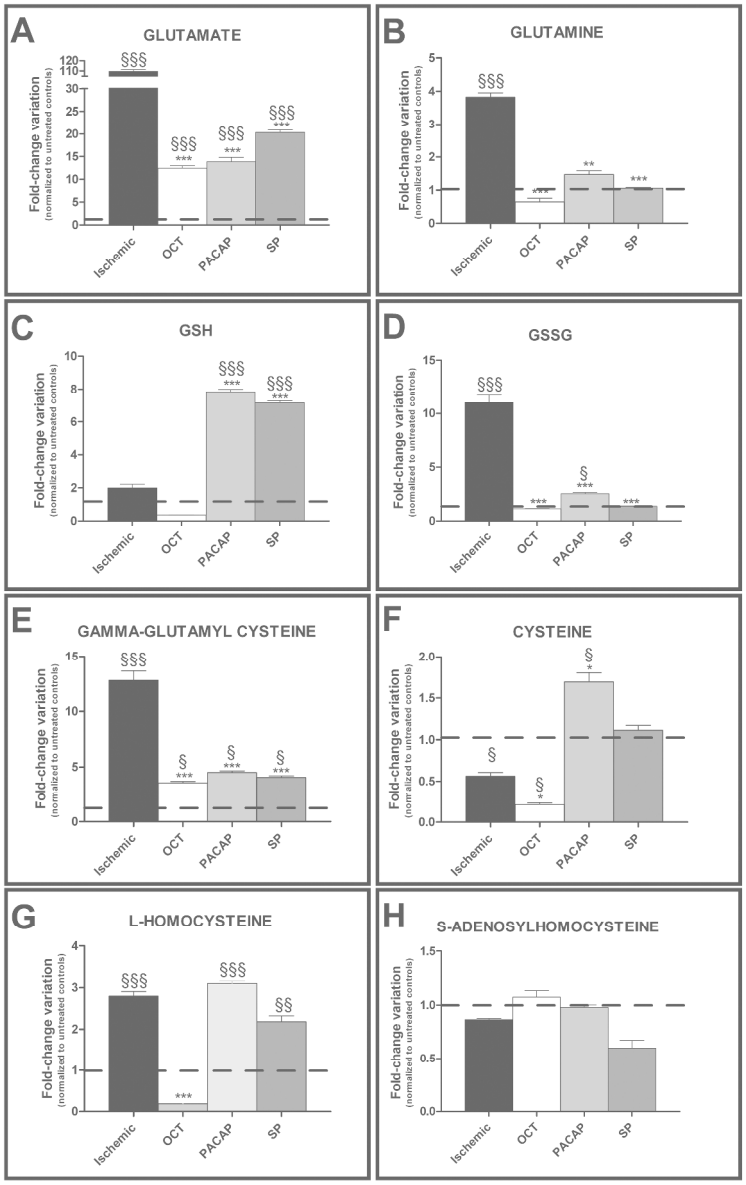

Fig. 3. GSH homeostasis and glutamate metabolism as assessed using untargeted metabolomic analyses. Values are expressed as mean ± SEM (n = 5) of the fold change over non-ischemic retinas (broken lines). §P < 0.01; §§P < 0.001; §§§P < 0.0001 against non-ischemic controls; *P <0.01; **P < 0.001; ***P < 0.0001 against untreated ischemic retinas, ANOVA.
200x317mm (600 x 600 DPI)

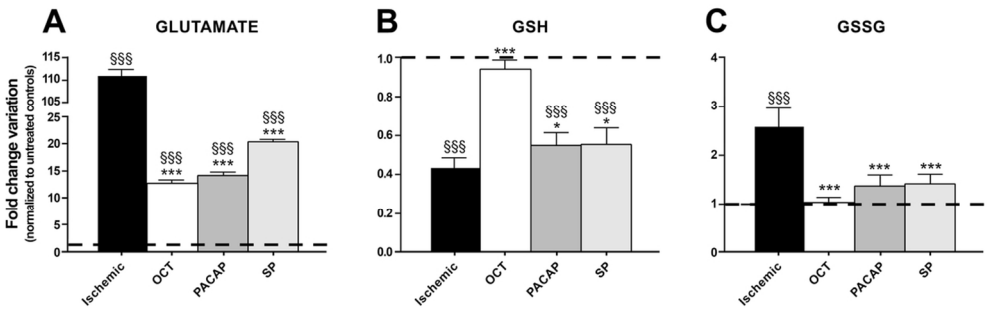

Fig. 4. Glutamate, GSH and GSSG levels detected through MRM targeted metabolomics. Values are expressed as mean ± SEM (n = 5) of the fold change over non-ischemic retinas (broken lines). §§§P < 0.0001 against non-ischemic controls; *P <0.01; ***P < 0.0001 against untreated ischemic retinas, ANOVA.
53x16mm (600 x 600 DPI)

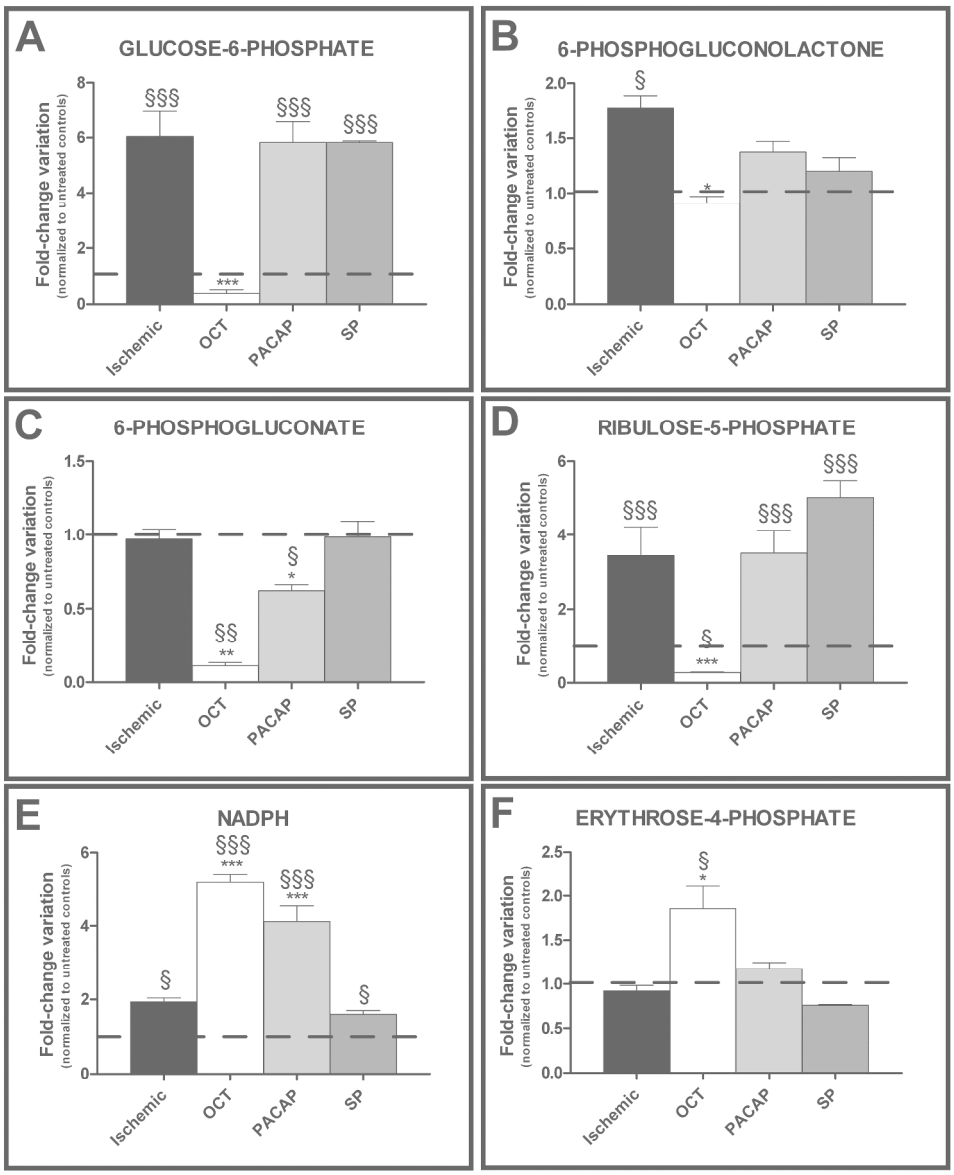

Fig. 5. PPP related metabolites, as assessed using untargeted metabolomic analyses. Values are expressed as mean ± SEM (n = 5) of the fold change over non-ischemic retinas (broken lines). §P < 0.01; §§§P < 0.0001 against non-ischemic controls; *P <0.01; **P < 0.001; ***P < 0.0001 against untreated ischemic retinas, ANOVA.
170x208mm (600 x 600 DPI)

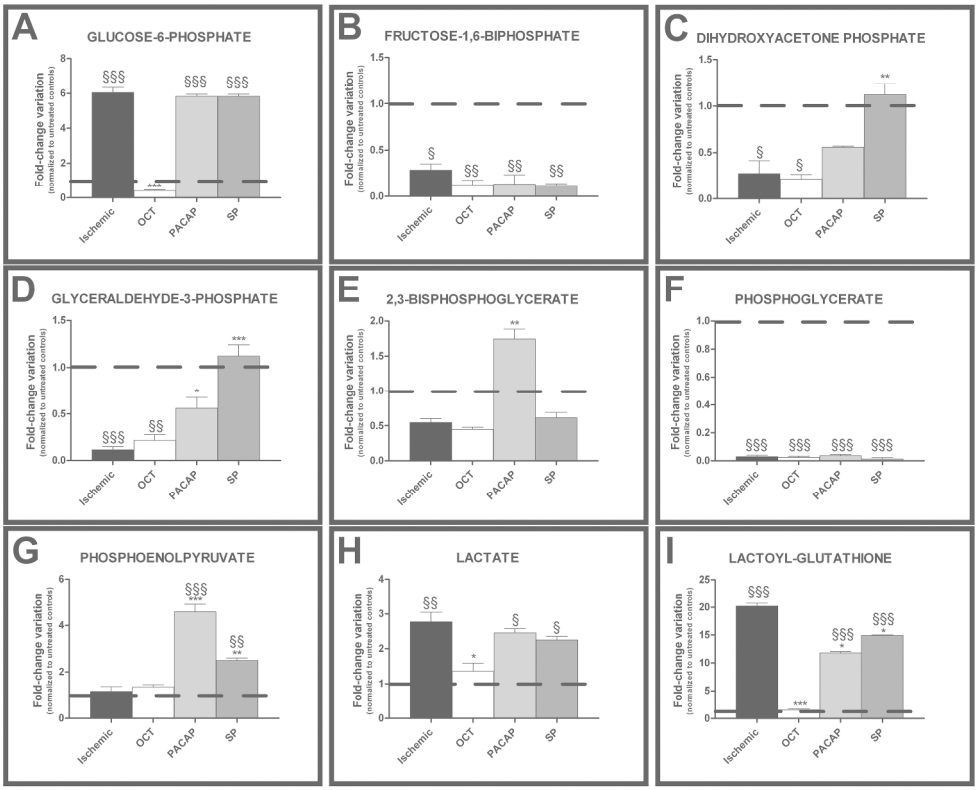

Fig. 6. Glycolytic metabolism through the Embden Meyerhof pathway, as assessed using untargeted metabolomic analyses. Values are expressed as mean ± SEM (n = 5) of the fold change over non-ischemic retinas (broken lines). §P < 0.01; §§§P < 0.0001 against non-ischemic controls; *P <0.01; **P < 0.001; ***P < 0.0001 against untreated ischemic retinas, ANOVA.
130x106mm (600 x 600 DPI)

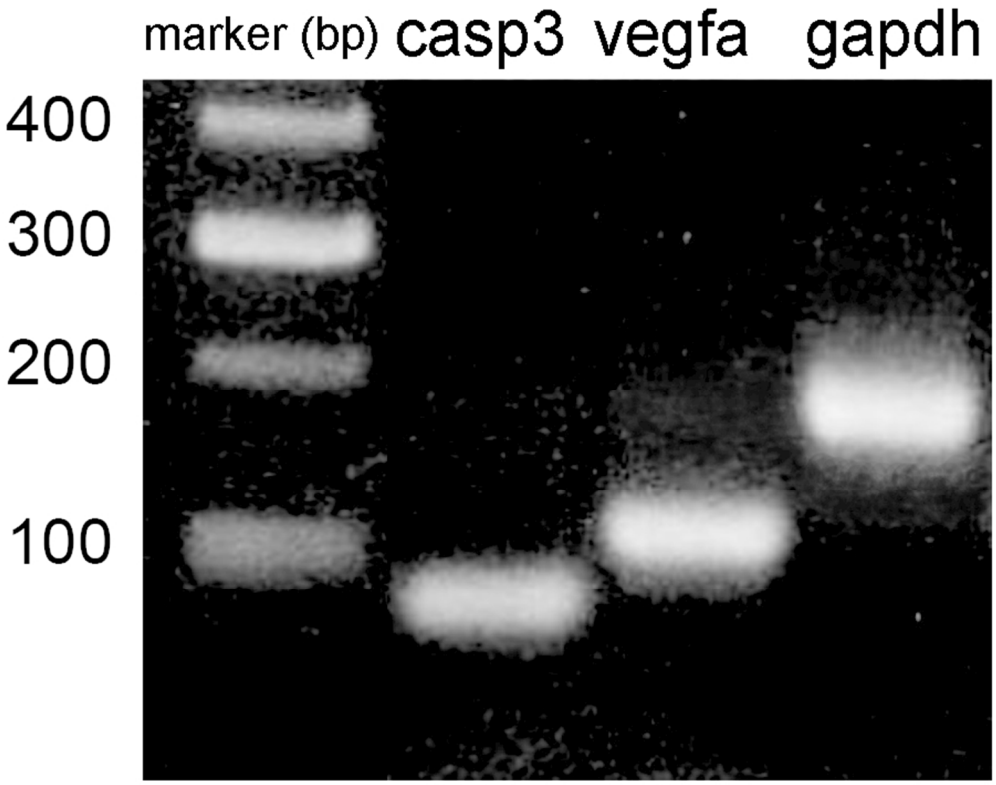

Suppl. Fig. 1. Representative gel electrophoresis of qPCR products.
76x60mm (300 x 300 DPI)

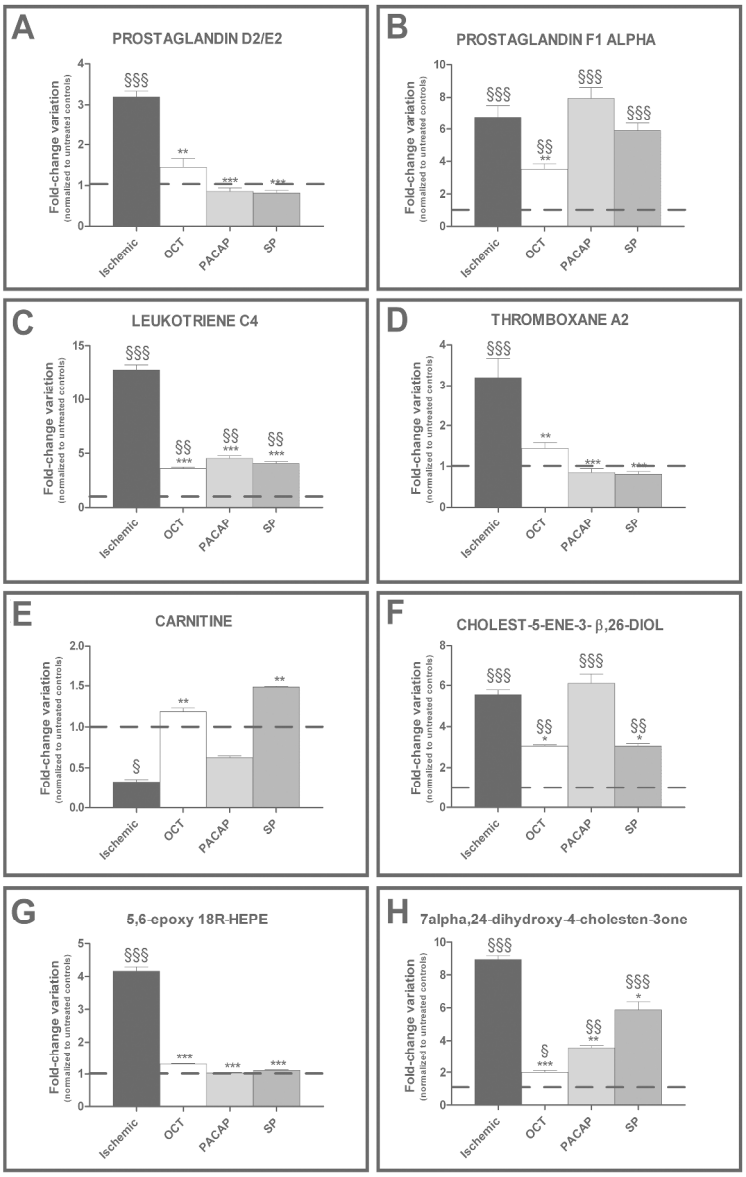

Suppl. Fig. 2. Lipid peroxidation and pro-inflammatory markers, as assessed using untargeted metabolomic analyses. Values are expressed as mean ± SEM (n = 5) of the fold change over non-ischemic retinas (broken lines). §P < 0.01; §§P < 0.001; §§§P < 0.0001 against non-ischemic controls; *P <0.01; **P < 0.001; ***P < 0.0001 against untreated ischemic retinas, ANOVA.
200x317mm (600 x 600 DPI)

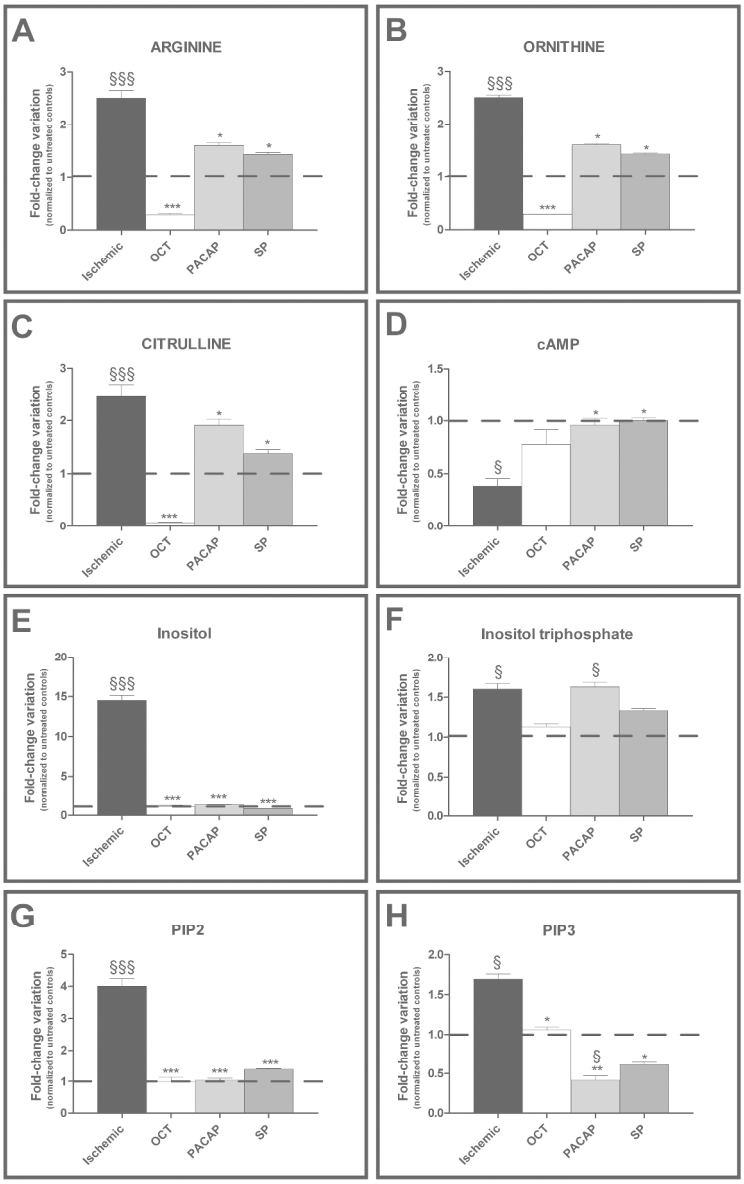

Suppl. Fig. 3. Arginine-citrulline-ornithine nitric oxide-related metabolism and secondary messenger metabolites (including cyclic AMP, inositol triphosphate, PIP2 and PIP3), as assessed using untargeted metabolomic analyses. Values are expressed as mean ± SEM (n = 5) of the fold change over non-ischemic retinas (broken lines). §P < 0.01; §§§P < 0.0001 against non-ischemic controls; *P <0.01; **P < 0.001; ***P < 0.0001 against untreated ischemic retinas, ANOVA.
200x317mm (600 x 600 DPI)

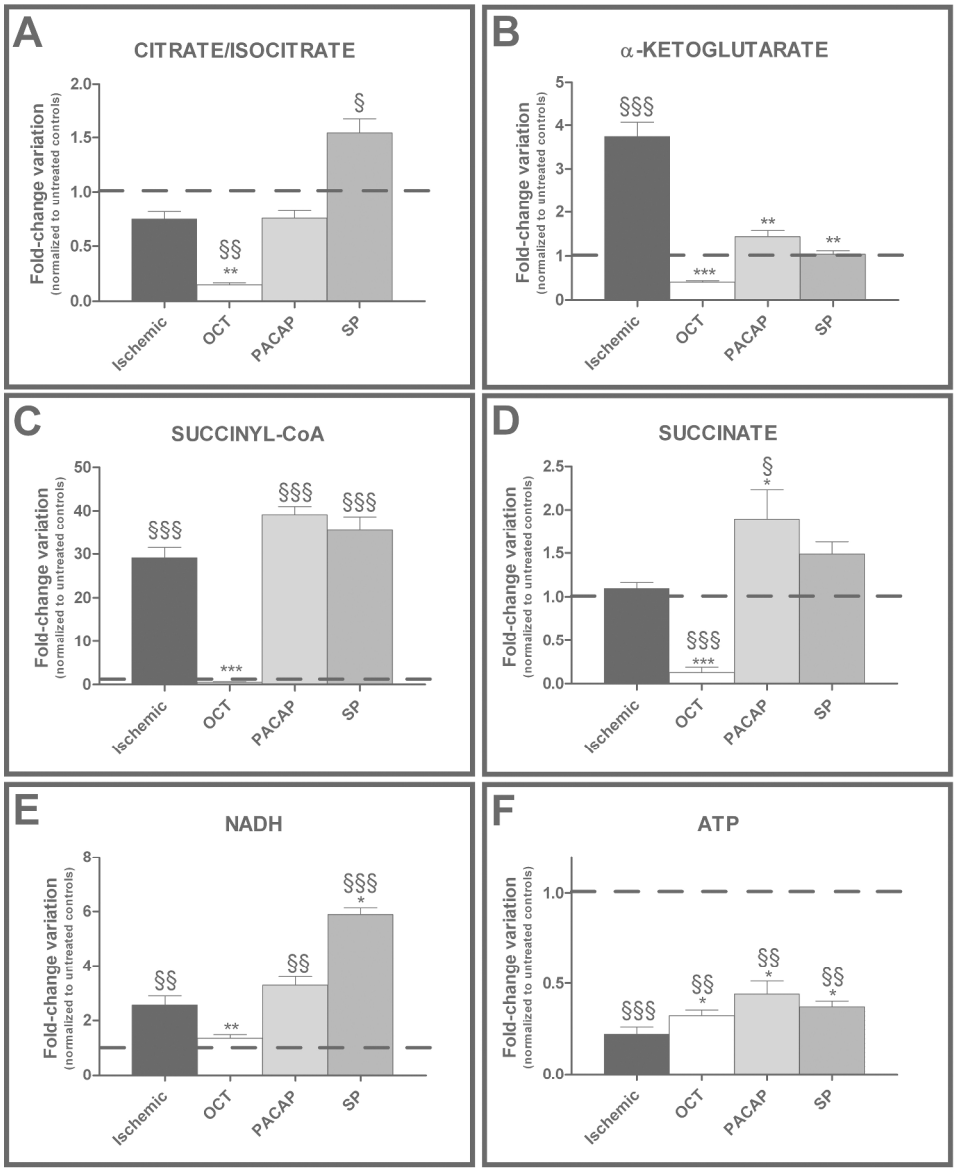

Suppl. Fig. 4. Krebs cycle metabolites, as assessed using untargeted metabolomic analyses. Values are expressed as mean ± SEM (n = 5) of the fold change over non-ischemic retinas (broken lines). §P < 0.01; §§§P < 0.0001 against non-ischemic controls; *P <0.01; **P < 0.001; ***P < 0.0001 against untreated ischemic retinas, ANOVA.
171x210mm (600 x 600 DPI)

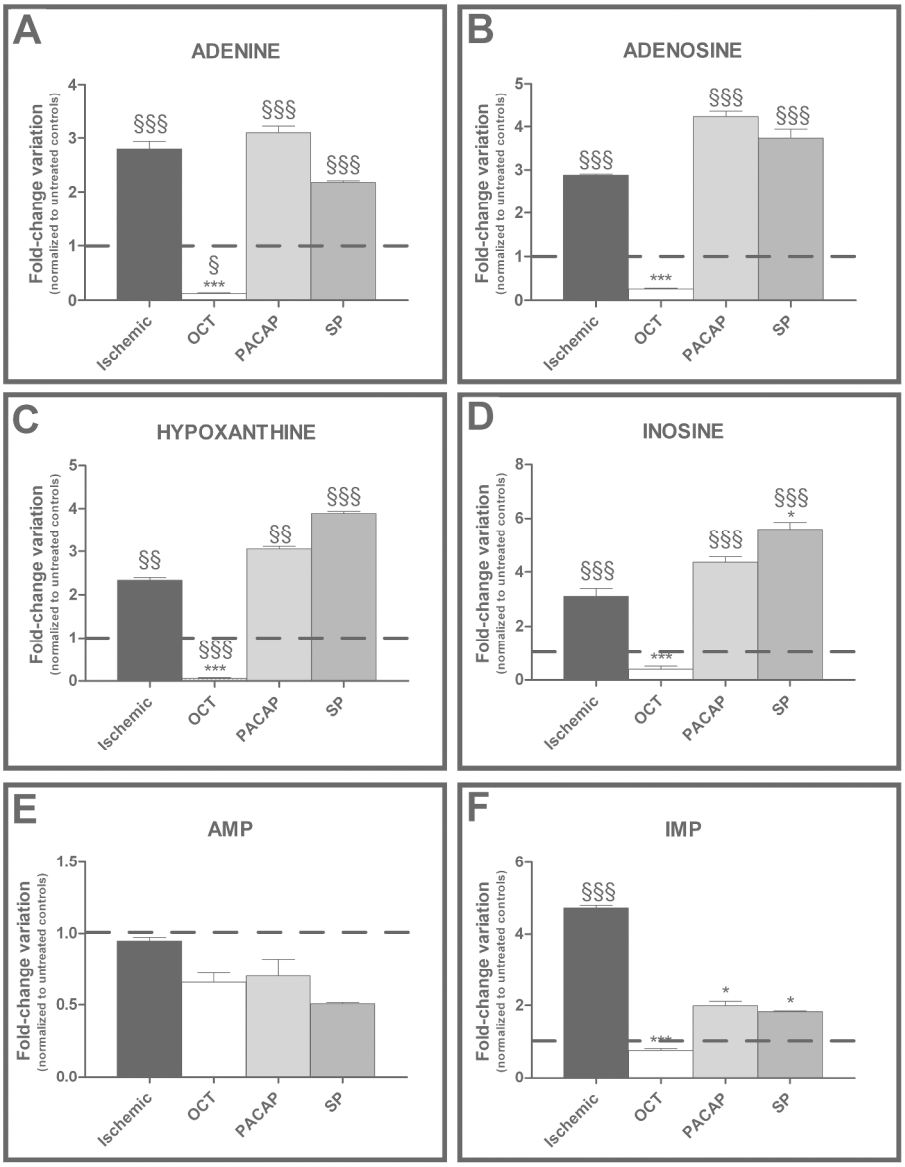

Suppl. Fig. 5. Purine metabolism, as assessed using untargeted metabolomic analyses. Values are expressed as mean ± SEM (n = 5) of the fold change over non-ischemic retinas (broken lines). §P < 0.01; §§§P < 0.0001 against non-ischemic controls; *P <0.01; ***P < 0.0001 against untreated ischemic retinas, ANOVA.
178x228mm (600 x 600 DPI)

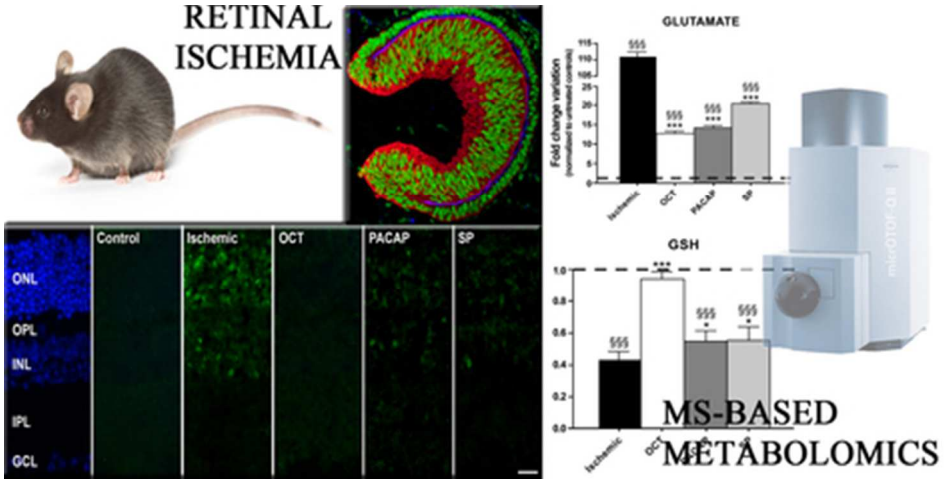

39x19mm (300 x 300 DPI)

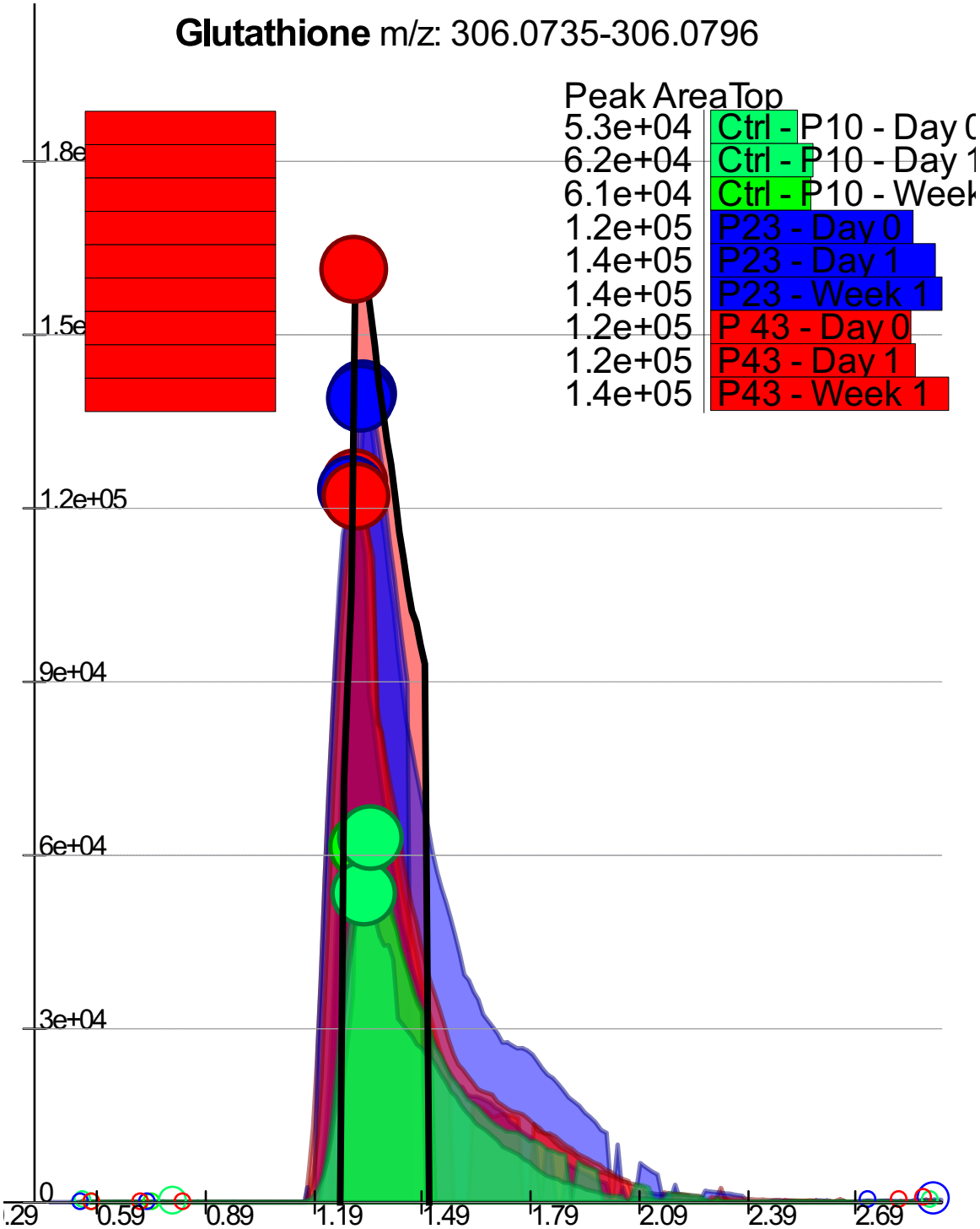
Glutathione m/z: 306.0735-306.0796
Peak AreaTop
5.3e+04 Ctrl - P10 - Day 0
6.2e+04 Ctrl - P10 - Day 1
6.1e+04 Ctrl - P10 - Week
1.2e+05 P23 - Day 0
1.4e+05 P23 - Day 1
1.4e+05 P23 - Week 1
1.2e+05 P 43 - Day 0
1.2e+05 P43 - Day 1
1.4e+05 P43 - Week 1
1.8e
1.5e
1.2e+05
9e+04
6e+04
3e+04
0
.29
0.59
0.89
1.19
1.49
1.79
2.09
2.39
2.69